J. Fluid Mech. (1990), *vol.* 220, *pp.* 309–337
Printed in Great Britain

Inviscid–viscous interaction on triple-deck scales in a hypersonic flow with strong wall cooling

By S. N. BROWN[1], H. K. CHENG[2] AND C. J. LEE[2]

[1] Department of Mathematics, University College London, Gower Street, London WC1E 6BT, UK

[2] Department of Aerospace Engineering, University of Southern California, Los Angeles, CA 90089-1191, USA

(Received 29 December 1989 and in revised form 30 March 1990)

Inviscid–viscous interaction in a high supersonic flow is studied on the triple-deck scales to delineate the wall-temperature influence on the flow structure in a region near a laminar separation. A critical wall-temperature range $O(T_w^*)$ is identified, in which the pressure–displacement relation governing the lower deck departs from that of the classical (Stewartson, Messiter, Neiland) formulation, and below which the pressure–displacement relation undergoes still greater changes along with drastic scale changes in the triple deck. The reduced lower-deck problem falls into three domains: (i) supercritical ($T_w^* \ll T_w$), (ii) transcritical ($T_w = O(T_w^*)$) and (iii) subcritical ($T_w \ll T_w^*$). Readily identified is a parameter domain overlapping with the Newtonian triple-deck theory of Brown, Stewartson & Williams (1975), even though the assumption of a specific-heat ratio approaching unity is not required here. Computational study of the compressive free-interaction solutions and solutions for a sharp-corner ramp are made for the three wall-temperature ranges. Finite-difference equations for primitive variables are solved by iterations, employing Newton linearization and a large-band matrix solver. Also treated in the program is the sharp-corner effect through the introduction of proper jump conditions. Comparison with existing numerical results in the supercritical T_w range reveals a smaller separation bubble and a more pronounced corner behaviour in the present numerical solution. Unlike an earlier comparison with solutions by interactive-boundary-layer methods for ramp-induced pressure with separation, the IBL results do approach closely the triple-deck solution at $Re = 10^8$ in a Mach-three flow, and the differences at $Re = 10^6$ may be attributed in part to the transcritical temperature effect. Examination of the numerical solutions indicates that separation and reattachment on a compressive ramp cannot be effectively eliminated/delayed by lowering the wall temperature, but lowering T_w drastically reduces the triple-deck dimension, and hence the degree of upstream influence.

1. Introduction

Significant inviscid–viscous interaction on a global scale brought about by the displacement effect is a well-known feature of laminar boundary layers at high Mach numbers (Stewartson 1955; Hayes & Probstein 1959; Moore 1964; Bogdonoff & Hammitt 1956; Cheng *et al.* 1961). There is yet another more universal character of an interacting laminar boundary layer not restricted to high-speed flows, which manifests itself in a much shorter scale, permits upstream influence and separation, and has been the focus of a vast number of theoretical studies (see for example

Lighthill 1953; Stewartson 1974, 1981; Stewartson & Williams 1969, 1973; Messiter 1979; Neiland 1969, 1971; Sychev 1974, 1987; Smith 1982, 1989). Central to these studies is the triple-deck theory which stipulates a three-tier structure made up of the lower, the main and the upper decks. This work is concerned with the triple-deck interaction problem in a boundary layer with a hypersonic outer flow.

For the problem at hand, one must distinguish cases in which the triple-deck interaction occurs in a flow field involving a strong global interaction from cases where the global interaction, if any, is weak. The strong and weak global interaction regimes correspond to both large and small values of a parameter $\chi \equiv M_1^3(C/Re)^{\frac{1}{2}}$, where C is a quantity depending on the viscosity–temperature relation and a reference temperature (see Hayes & Probstein 1959). For a χ of unit order or much larger, the triple-deck description is inapplicable, with the exception of a version under a Newtonian approximation which requires the specific-heat ratio to be close to unity, i.e. $\gamma \to 1$ (Brown, Stewartson & Williams 1975). The present analysis addresses the triple-deck problem in the weak global interaction regime ($\chi \ll 1$), with the effect of a strong wall cooling as the main focus. As it turns out, the range of T_w/T_0 need not be too low for its effects to be manifested significantly in an application.

Unique to the present study is a characteristic wall-temperature level T_w^* determined principally by χ, hence by the Mach and Reynolds numbers (to be precisely defined later). The analysis identifies three distinct wall-temperature ranges:

(i) Supercritical: $T_w \gg T_w^*$,

(ii) Transcritical: $T_w = O(T_w^*)$,

(iii) Subcritical: $T_w^* \gg T_w$.

The work of Lighthill (1953), Stewartson (1974, 1981), Stewartson & Williams (1969, 1973), Messiter (1979), Neiland (1969, 1971), Sychev (1974, 1987), and Smith (1982, 1989) may be considered as a special limit $T_w/T_w^* \to \infty$ of the supercritical range.

Significant departure from this limit occurs in the transcritical range where the pressure–displacement interaction law for the lower deck needs to be modified. Greater departure occurs in the subcritical range where strong wall cooling brings about a drastic alteration in the pressure–displacement relation and in the relative scales which, with the trivial exception of the upper-deck height, become independent of the Mach and Reynolds numbers, being principally determined by T_w/T_0. The entry of T_w/T_0 into the scalings, particularly into the 'ϵ' of the basic theory, should prove to be helpful in application, since ϵ will be rendered smaller for a lower wall temperature, and hence the asymptotic analysis more accurate.

Although the basic premise in the triple-deck analysis of Brown *et al.* (1975) ($\gamma - 1 \ll 1$) and in the present study ($T_w/T_0 \ll 1$) are quite different, their governing equations in reduced variables are virtually the same. Specializing to the parameter domain where both $(\gamma - 1)$ and T_w/T_0 are small, a domain of applicability common to both analyses does exist. (For the restricted domain of small $(\gamma - 1)$, T_w/T_0 and χ, the present work could be regarded as a reformulation for Brown *et al.* (1975), providing an improvement in approximation as well as in the rationale for the ordering used in the formulation/derivation.)

The triple-deck structure is generally inapplicable in a regime where χ is not (asymptotically) small, and the treatment with $(\gamma - 1) \ll 1$ (Brown *et al.* 1975) appears to be the only viable approach for large χ to date. The reduced problem of Brown *et al.* (1975) has been computationally studied for the supersonic boundary layer over a ramp by Rizzetta, Burggraf & Jenson (1978) and for the case of free

interaction by Gajjar & Smith (1983), where the Newtonian model of Brown *et al.* (1975) is simply referred to as that of a 'hypersonic triple-deck'. One outstanding result accomplished in Brown *et al.* (1975) is perhaps its reconciliation with the eigensolution to the perturbation series from the Lees–Stewartson similarity solution (Stewartson 1955; Hayes & Probstein 1959; Moore 1964) for an infinite χ, first uncovered by Neiland (1970), and more generally studied by Werle, Dwoyer & Hankey (1973) and by Brown & Stewartson (1975).

The present work represents a development for small χ, allowing also for small T_w/T_0. Contributions from several pressure corrections absent from the theory of Lighthill (1953), Stewartson (1974, 1981), Stewartson & Williams (1969, 1973), Messiter (1979), Neiland (1969, 1971), Sychev (1974, 1987), and Smith (1982, 1989) find themselves ranked with the leading approximation in the transcritical and subcritical wall-temperature ranges. The centrifugal-force effect controlling the pressure variation across the main deck belongs, however, to a higher order. At still lower wall temperatures, nevertheless, this effect could become of first-order importance and will be considered in a separate work.

Since large differences in temperature level can exist between the lower and the main deck, a nonlinear viscosity–temperature relation ($\mu \propto T^{\omega}$) is allowed and preferred over the linear one ($\mu \propto T$) adopted in most works. This should permit a physically more appropriate framework for matching correctly the lower and the main decks and for proper scalings and ordering in the approximations.

In a relatively recent work on some features of the transcritical boundary layer interaction and separation, V. Ya. Neiland (1989, private communication) has noted and studied the wall-cooling effects, distinguishing also a transcritical wall-temperature range from other domains. The correspondence between these domains and the three temperature ranges of the present work is not very apparent. Unlike the following analysis, the equations in the main and upper decks therein are nonlinear with rather interesting transition behaviour. In passing, we note a rather comprehensive review by Kluwick (1987) on development in the triple-deck theory, where more recent works in supersonic cases are discussed.

The questions of whether, and in what manner, a lowering of wall temperature may actually alter the physical scales and features of a triple-deck separation/reattachment cannot be answered unambiguously without the support of concrete solutions from the computational study. Whereas the lower-deck governing equations in reduced variables obtained below can be identified with the corresponding Newtonian system in Brown *et al.* (1975) and in Rizzetta *et al.* (1978), existing results are far from answering/resolving the issues of interest. In the present study, a finite-difference equation system in primitive variables was solved by a relaxation method, using spatial central differences, Newton linearization and a large-band matrix solver for each iteration. Solutions have been obtained for compressive free interactions and for sharp-corner ramps, with wall temperatures in the three different ranges. The program is implemented by a unique treatment of the sharp-corner effect in the form of jump conditions across the lower deck. Studies establishing mesh-size convergence and comparing the present work with existing numerical results based on the triple-deck analyses (Brown *et al.* 1975; Rizzetta *et al.* 1978; Jenson 1977; Gajjar & Smith 1983; Williams 1975) and from the interactive boundary-layer (IBL) method (Werle & Vatsa 1974) are made. The comparison appears to suggest that some of the discrepancies between triple-deck and IBL solutions may be attributed to the transcritical wall temperature and other effects unaccounted for in the standard work. From the following development, the effect

of the interaction on the surface heating rate will be seen to be significant but can be separately treated. This work was presented in the Conference of Prediction and Exploitation of Separated Flow (Brown, Cheng & Lee 1989).

2. Triple-deck analysis of a compressible boundary layer

We consider the boundary layer in a steady, plane, compressible flow of a calorically perfect gas. The Mach number at its outer edge is assumed to be very high ($M_1 \gg 1$). The conventional boundary-layer coordinates x and y, with corresponding velocity components u and v, are adopted. The variables x, y, u and v are non-dimensionalized by a global streamwise length L, a typical boundary-layer thickness δ, and the representative outer-edge tangential and normal velocities U_1 and $\delta U_1/L$, respectively. The two velocity components so normalized are denoted by $\bar{u}$ and $\bar{v}$. The non-dimensional density $\bar{\rho}$ is normalized by the representative outer-edge value ρ_1, the pressure $\bar{p}$ by $\rho_1 U_1^2 \epsilon_0^2$, the temperature $\bar{T}$ by $\frac{1}{2}U_1^2/C_p$, and the total enthalpy $\bar{H}$ by $\frac{1}{2}U_1^2$, where C_p is the specific heat at constant pressure and ϵ_0 is a parameter to be chosen from the largest among M_1^{-1}, δ/L and α^* (a typical surface slope or ramp angle). The temperature $\bar{T}$ so normalized is recognized as the variable S in Brown *et al.* (1975), being slightly greater than the temperature ratio based on the stagnation temperature T_0 by a factor $(1+(2/\gamma-1)M_1^{-2})$. In these variables, the equation of state gives

$$\epsilon_0^2 \bar{p} = \frac{\gamma-1}{2\gamma}\bar{\rho}\bar{T}. \tag{2.1}$$

Although the ϵ_0 gauging the global pressure difference will be taken later to be $1/M_1$, restricting the application principally to the regime of a low χ, this assumption is unnecessary until (2.59). Therefore, the substitution $\epsilon_0 = 1/M_1$ will not be made at this stage, so that subsequent extensions involving other types of external flows can be more readily carried out. Note that the results obtained are applicable also to a hypersonic wedge flow involving a very strong shock, as long as the subscript '1' is used to refer to the condition upstream of the triple deck behind the shock.

A constant Prandtl number of the order unity is assumed; the viscosity–temperature relation is represented by a power law

$$\mu \propto T^{\omega} \tag{2.2}$$

for reasons noted earlier. The formulation also allows the option of a model fluid based on a linear viscosity–temperature relation with a reference viscosity $\mu_* \equiv \mu(T_*)$ at a reference temperature T_* (Cheng *et al.* 1961)

$$\frac{\mu}{\mu_*} = \left(\frac{T}{T_*}\right) \tag{2.3}$$

which would result in a slightly different definition for the interaction parameter χ (see below). The analysis will be presented for the exponent of (2.2) in the range

$$\tfrac{1}{2} < \omega \leqslant 1. \tag{2.4}$$

A comment will be given later for the case $\omega = \frac{1}{2}$.

2.1. *The boundary layer on global scales*

We assume that a triple-deck structure can be embedded in an upstream global structure furnished by the boundary layer. It is convenient to work with the renormalized Dorodnitsyn variables

$$\xi = x, \quad \eta = A_0 \int_0 \bar{\rho}\, \mathrm{d}y, \tag{2.5}$$

with

$$A_0 \equiv \frac{\delta}{L}(\epsilon_0 M_1)^{-1}\left(\frac{Re}{\gamma C_0}\right)^{\frac{1}{2}}, \tag{2.6}$$

$$Re \equiv \frac{\rho_1 U_1 L}{\mu_1}, \quad C_0 \equiv \frac{\mu_0' T_1}{\mu_1 T_0'}, \tag{2.7}$$

where $\mu_0' = \mu(T_0')$ and $T_0' = T_0/(1+(2/\gamma-1)M_1^{-2})$, and the stream function

$$\Psi = A_0 \psi, \tag{2.8}$$

with $\partial\psi/\partial x = -\bar{\rho}\bar{v}$ and $\partial\psi/\partial y = \bar{\rho}\bar{u}$. The governing equations of the boundary layer can be transformed into a nearly incompressible form, subject to errors of the order of $(\delta/L)^2$,

$$\bar{U}\bar{U}_\xi + \bar{V}\bar{U}_\eta + \frac{\gamma-1}{2\gamma}\bar{T}(\ln\bar{p})_\xi = \bar{p}(\bar{N}\bar{U}_\eta)_\eta, \tag{2.9}$$

$$\bar{U}\bar{H}_\xi + \bar{V}\bar{H}_\eta = \bar{p}\left\{\frac{\bar{N}}{Pr}[\bar{H}_\eta - (1-Pr)(\bar{U}^2)_\eta]\right\}_\eta, \tag{2.10}$$

$$\bar{U}_\xi + \bar{V}_\eta = 0, \tag{2.11}$$

where subscripts ξ and η signify partial derivatives and

$$\bar{N} \equiv \frac{\mu}{\mu_0'}\frac{T_0'}{T} = (\bar{T})^{\omega-1}; \tag{2.12}$$

and

$$\bar{T} = \bar{H} - \bar{U}^2,$$

$$\bar{U} = \frac{\partial\Psi}{\partial\eta} = \bar{u}, \quad \bar{V} = -\frac{\partial\Psi}{\partial\xi}(\neq \bar{v}). \tag{2.13}$$

Note that $\bar{p}$, $\bar{H}$ and $\bar{T}$ are variables non-dimensionalized by scales indicated at the beginning of this section. If the model-fluid option of (2.3) is to be used, (2.5)–(2.13) remain unchanged except for the replacement of C_0 of (2.7) by

$$C \equiv \frac{\mu_*}{\mu_1}\frac{T_1}{T_*}. \tag{2.14}$$

Associated with (2.9)–(2.11) are the usual boundary conditions

$$\bar{U} = \bar{U}_e(\xi), \quad \bar{H} = \bar{H}_e(\xi), \quad \eta \to \infty, \tag{2.15}$$

$$\bar{U} = 0, \quad \bar{V} = 0, \quad \bar{H} = \bar{T}_w \equiv s_w, \quad \eta \to 0. \tag{2.16}$$

Henceforth, we shall denote $\bar{T}_w = T_w(1+(2/\gamma-1)M_1^{-2})/T_0$ by s_w. Note that, whereas $\bar{U}_e$ can be taken to be unity, $\bar{H}_e$ does not generally approach unity except in the limit $M_1 \to \infty$.

Essential to the triple-deck analysis are the non-vanishing heat flux and shear stress at the wall in the original boundary-layer solution, which are controlled by both s_w and ω. These quantities are the products of $\bar{N}$ with gradients of $\bar{H}$ and $\bar{U}$ next to the wall. Let

$$\bar{\lambda}_T \equiv \left(\bar{N}\frac{\partial\bar{H}}{\partial\eta}\right)_w, \quad \bar{\lambda}_u \equiv \left(\bar{N}\frac{\partial\bar{U}}{\partial\eta}\right)_w. \tag{2.17}$$

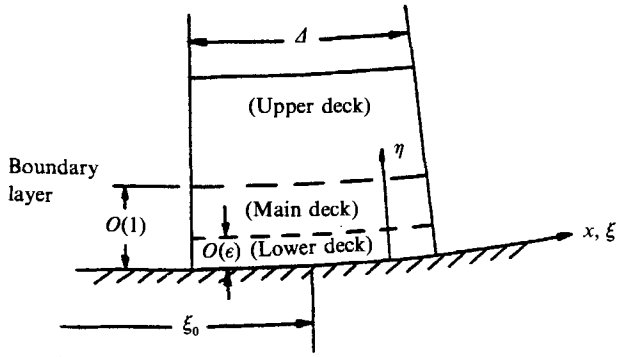

FIGURE 1. Illustration of a triple-deck structure of the interaction zone with relative scales shown in Dorodnitsyn variables.

The boundary-layer equations (2.9)–(2.16) admit a solution behaviour near the wall for finite, non-vanishing $\bar{\lambda}_T$ and $\bar{\lambda}_u$:

$$\bar{T} \sim (s_w^\omega + \omega \bar{\lambda}_T \eta)^{\frac{1}{\omega}}, \tag{2.18}$$

$$\bar{U} \sim \bar{\lambda}_u \int_0 \bar{T}^{1-\omega} \mathrm{d}\eta, \tag{2.19}$$

subject to relative errors of orders $\bar{U}^2\eta$ and $s_w\eta$, respectively. It follows that the first and second partial derivatives may also be evaluated in terms of $\bar{\lambda}_u$, $\bar{\lambda}_T$ and s_w as

$$\left(\frac{\partial \bar{T}}{\partial \eta}\right)_w = s_w^{1-\omega}\bar{\lambda}_T, \quad \left(\frac{\partial \bar{U}}{\partial \eta}\right)_w = s_w^{1-\omega}\bar{\lambda}_u, \tag{2.20}$$

$$\left.\begin{aligned} \left(\frac{\partial^2 \bar{T}}{\partial \eta^2}\right)_w &= (1-\omega)\, s_w^{1-2\omega}\bar{\lambda}_T^2 - 2Pr\bar{\lambda}_u^2 s_w^{2-2\omega}, \\ \left(\frac{\partial^2 \bar{U}}{\partial \eta^2}\right)_w &= (1-\omega)\, s_w^{1-2\omega}\bar{\lambda}_T\bar{\lambda}_u + \frac{\gamma-1}{2\gamma\bar{p}} s_w^{2-\omega}\frac{\mathrm{d}}{\mathrm{d}\xi}\ln\bar{p}. \end{aligned}\right\} \tag{2.21}$$

If one denotes the wall values of the gradients $\bar{H}_\eta$ and $\bar{U}_\eta$ by

$$\lambda_T \equiv \left(\frac{\partial \bar{H}}{\partial \eta}\right)_w, \quad \lambda_u \equiv \left(\frac{\partial \bar{U}}{\partial \eta}\right)_w, \tag{2.22}$$

λ_T can be related to $\bar{\lambda}_T$, and λ_u to $\bar{\lambda}_u$, by

$$\lambda_T = s_w^{1-\omega}\bar{\lambda}_T, \quad \lambda_u = s_w^{1-\omega}\bar{\lambda}_u. \tag{2.23}$$

Note that λ_T and λ_u vanish with s_w like $s_w^{1-\omega}$. The results (2.18)–(2.23) are valid as long as $\eta \ll s_w^\omega$, and $\frac{1}{2} \leqslant \omega \leqslant 1$. Subsequent analysis will establish that in the lower deck η is comparable with the parameter ϵ which gauges the perturbation of $\bar{U}$ in the main deck, and that $\epsilon \ll s_w^\omega$. Therefore these behaviours in the main deck can be assumed in the matching with the lower-deck solution later.

We shall proceed to formulate the triple-deck problem, using the normalized Dorodnitsyn variable η as the transverse coordinate for the main deck, implying of course that the main deck has the same transverse scale as the global boundary layer. An illustration of the three-tier structure in question is sketched in figure 1 where several notations and definitions for various relative lengthscales and coordinates are

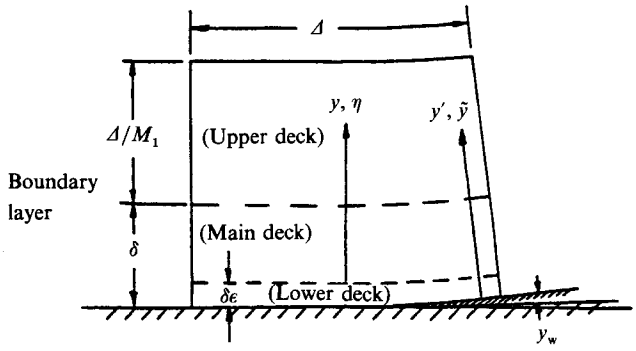

FIGURE 2. Illustration of a triple-deck structure with relative scales in boundary-layer coordinates. Note that the surface/ramp angle change is assumed to be small enough that the surface elevation measured from local Cartesian coordinates does not rise above the lower deck.

also indicated. The physical extent of the upper deck may be taken to be of the order Δ/M_1 (cf. figure 2), which is not crucial in the present study and is of the order of δ/ϵ in the supercritical case. The (physical) thickness of the upper deck is in fact comparble with that of the main deck in the transcritical range, and this could cause problems in matching of upper- and main-deck solutions. However, this ambiguity does not arise in the following development which employs the Dorodnitsyn variable η.

2.2. *The main deck*

Let the triple-deck structure be centred at $\xi = \xi_0$. We shall introduce a new streamwise variable for the triple deck based on the shorter lengthscale Δ,

$$\xi' \equiv \frac{\xi - \xi_0}{\Delta}. \tag{2.24}$$

Thus, apart from the variable η, the main-deck structure is described by two streamwise variables: a global one, ξ, describing the boundary-layer solution and the new variable ξ' describing the steeper gradient provoked by the interaction. Let us assume an expansion for the tangential velocity

$$\bar{U} = U_0(\xi, \eta; s_w) + \epsilon U_1(\xi', \eta; \xi_0, s_w) + \epsilon_p U_p(\xi', \xi, \eta; \xi_0, s_w) + \epsilon_p' U_{p1} + \epsilon^2 U_2 + \ldots, \tag{2.25}$$

where ϵ gauges principally the $\bar{U}$-perturbation, as noted earlier; ϵ_p and ϵ_p' are small parameters gauging the displacement–pressure and centrifugal–pressure corrections, respectively, assumed to be of orders higher than ϵ. The wall-temperature ratio s_w, though small in most instances of interest, is not expanded out until a later stage when appropriate relations among s_w, ϵ and ϵ_p will be assigned, depending on the parameter domain delineated. Similar forms are assumed for the total enthalpy $\bar{H}$ and temperature $\bar{T}$. The transverse velocity $\bar{V}$ corresponding to the $\bar{U}$ of (2.25) must take a form to satisfy the continuity equation (2.11):

$$\bar{V} = V_0(\xi, \eta; s_w) + (\epsilon/\Delta)\, V_1(\xi', \eta : \xi_0, s_w) + (\epsilon/\Delta)\, V_p(\xi', \xi, \eta; \xi_0, s_w) + \ldots, \tag{2.26}$$

where, to be sure, $\epsilon V_1/\Delta$ and $\epsilon_p V_p/\Delta$ are expected to be of an order lower than V_0. The issue of uniformity does not arise in this instance since the higher-order remainder can be established, as in the standard triple-deck theory (see Stewartson 1974). The main-deck expansion for the pressure is

$$\bar{p} = P_0(\xi) + \epsilon_p P_1(\xi', \eta; \xi_0, s_w) + \epsilon_p' P_{p1} + \epsilon^2 P_2 + \ldots. \tag{2.27}$$

The subscript '1' on P could have been replaced by 'p' to be consistent with the usage of U_p, H_p, etc. Unlike the ordering stipulated in the standard theory, ϵ^2 will not rank equally with ϵ_p, owing to the change in the relative sizes of certain terms brought about by a vanishing s_w. In fact, the centrifugal effect will give rise to a correction with magnitude intermediate between ϵ_p and ϵ^2, to be confirmed later. In this study, the outer (global) flow is taken to be uniform upstream; it follows that $P_0 = (M_1\epsilon_0)^2/\gamma$. The work presented below will be limited to domains where ϵ_p' and ϵ^2 are of order higher than ϵ_p; the explicit criteria delimiting the domain studied will be given later. The $T_0(\eta)$ in (2.29), (2.31)–(2.35) below is the leading term in the expansion of the normalized temperature distribution $\bar{T}$, not to be confused with the free-stream stagnation temperature T_0.

Substituting the foregoing expansions into the Navier–Stokes equations yields a system of first-order partial differential equations (PDE) in ξ' and η for U_1, V_1 and H_1 or T_1, which yields the main-deck result at the level of ϵ:

$$V_1 = -A'(\xi')\,U_0(\eta), \quad U_1 = A(\xi')\,U_0'(\eta), \tag{2.28}$$

$$H_1 = A(\xi')\,H_0'(\eta), \quad T_1 = A(\xi')\,T_0'(\eta), \tag{2.29}$$

where the prime on $U_0(\eta)$, $H_0(\eta)$ and $T_0(\eta)$ signifies a derivative, and the parametric dependence of the results on s_w and ξ_0 is understood. Here, U_0, H_0 and T_0 are the global boundary-layer solutions; from (2.28) and (2.29) one may infer that the function $-A(\xi')$, yet to be determined, is manifested as a local displacement effect to the main and the upper decks, but the non-slip wall conditions cannot be satisfied and a sublayer – the lower deck – is needed. These are familir results. Nevertheless, the simplistic form (2.29) for T_1 will be decisive in bringing about a far-reaching wall influence on the triple deck.

As pointed out earlier, the ϵ_p' is determined from the normal momentum equation to be

$$\epsilon_p' = \tfrac{1}{2}(\gamma-1)\,\gamma(\epsilon_0 M_1)^{-2}A^{-2}\epsilon C_0 M_1^4 Re^{-1}, \tag{2.30}$$

with which

$$\frac{\partial P_{p1}}{\partial \eta} = -U_0^2(\eta)\,T_0(\eta)\,A''(\xi'). \tag{2.31}$$

At the level of ϵ_p, the corresponding PDE's provide a less simplistic solution form:

$$P_1 = P_1(\xi'), \tag{2.32}$$

$$V_p = U_0(\eta)\left\{\tfrac{1}{2}(\gamma-1)(\gamma P_0)^{-1}P_1'(\xi')[-D_1\eta^{-1}+D_2\ln\eta + \int_0 (T_0 U_0^{-2} - D_1\eta^{-2} - D_2\eta^{-1})\,\mathrm{d}\eta] - A_p'(\xi')\right\}, \tag{2.33}$$

$$U_p = U_0'(\eta)\left\{A_p(\xi') - \tfrac{1}{2}(\gamma-1)(\gamma P_0)^{-1}P_1(\xi')[-D_1\eta^{-1}+D_2\ln\eta + \int_0 (T_0 U_0^{-2} - D_1\eta^{-2} - D_2\eta^{-1})\,\mathrm{d}\eta]\right\} - \tfrac{1}{2}(\gamma-1)(\gamma P_0)^{-1}P_1 T_0 U_0^{-1}, \tag{2.34}$$

$$T_p = -T_0'(\eta)\left\{-A_p(\xi') + \tfrac{1}{2}(\gamma-1)(\gamma P_0)^{-1}P_1(\xi')[-D_1\eta^{-1}+D_2\ln\eta + \int_0 (T_0 U_0^{-2} - D_1\eta^{-2} - D_2\eta^{-1})\,\mathrm{d}\eta]\right\} + (\gamma-1)(\gamma P_0)^{-1}P_1 T_0, \tag{2.35a}$$

where

$$D_1 \equiv \frac{s_w^{2\omega-1}}{\bar{\lambda}_u^2}, \quad D_2 \equiv \frac{\omega\bar{\lambda}_T}{s_w^{1-\omega}\bar{\lambda}_u^2} - \tfrac{1}{2}(\gamma-1)(\gamma P_0)^{-1}\frac{s_w^{2\omega}}{\bar{\lambda}_u^3}\frac{\mathrm{d}}{\mathrm{d}\xi}\ln P_0, \tag{2.35b, c}$$

and $P_1(\xi')$ and $A_p(\xi')$ are functions to be determined. The results (2.28)–(2.35), as well as results for the levels ϵ_p' and ϵ^2 not presented here, pertain to a perturbation solution of an inviscid, nearly parallel, rotational flow, their viscous corrections belong to the order Δ higher, as may be inferred from (2.9) and (2.10). As in the classical theory, Δ will be shown to be much smaller than ϵ and ϵ_p. The key to the lower-deck analysis is the behaviour of $\bar{U}$ and $\bar{T}$ based on (2.28)–(2.35) in the inner limit $\eta \to 0$:

$$\begin{aligned}
\frac{\bar{U}}{s_w^{1-\omega}\epsilon\bar{\lambda}_u} \sim{}& \frac{\eta}{\epsilon}+A(\xi')+\frac{\epsilon}{s_w^{\omega}}\bar{\lambda}_T\tfrac{1}{2}(1-\omega)\left[\left(\frac{\eta}{\epsilon}\right)^2+2A\frac{\eta}{\epsilon}\right]\\
&+\epsilon s_w\frac{\frac{1}{4}(\gamma-1)}{\bar{\lambda}_u}(\gamma P_0)^{-1}\frac{\mathrm{d}}{\mathrm{d}\xi}\ln P_0\left[\left(\frac{\eta}{\epsilon}\right)^2+2A\left(\frac{\eta}{\epsilon}\right)\right]\\
&+\frac{\epsilon_p}{s_w^{1-\omega}\epsilon}\left\{s_w^{1-\omega}A_p(\xi')-\tfrac{1}{2}(\gamma-1)(\gamma P_0)^{-1}\bar{\lambda}_u^{-2}\bar{\lambda}_T P_1(\xi')\right.\\
&\left.\times\left[\omega\ln\epsilon+\omega\ln\left(\frac{\eta}{\epsilon}\right)+\frac{3\omega-1}{2}\right]\right\}\\
&+\frac{\epsilon_p}{\epsilon}\left\{[\tfrac{1}{2}(\gamma-1)(\gamma P_0)^{-1}]^2\frac{P_1}{\bar{\lambda}_u^3}\frac{\mathrm{d}}{\mathrm{d}\xi}\ln P_0\left[s_w^{2\omega}\left(\ln\epsilon+\ln\frac{\eta}{\epsilon}\right)+\tfrac{3}{2}\right]\right\}, \qquad (2.36)\\
\frac{\bar{T}}{s_w} \sim{}& 1+\frac{\epsilon}{s_w^{\omega}}\bar{\lambda}_T\left[\frac{\eta}{\epsilon}+A(\xi')\right]+\left(\frac{\epsilon}{s_w^{\omega}}\right)^2\tfrac{1}{2}(1-\omega)\bar{\lambda}_T^2\left[\left(\frac{\eta}{\epsilon}\right)^2+2A\frac{\eta}{\epsilon}\right]\\
&-\epsilon^2 Pr\,\bar{\lambda}_u^2 s_w^{1-2\omega}\left[\left(\frac{\eta}{\epsilon}\right)^2+2A\left(\frac{\eta}{\epsilon}\right)\right]\\
&+\frac{\epsilon_p}{s_w^{1-\omega}\epsilon}\left\{\tfrac{1}{2}(\gamma-1)(\gamma P_0)^{-1}\frac{\bar{l}_T}{\bar{\lambda}_u^2}P_1(\xi')\left[\frac{\epsilon}{\eta}-\frac{\epsilon}{s_w^{\omega}}\omega\bar{\lambda}_T\left(\ln\epsilon+\ln\frac{\eta}{\epsilon}\right)\right]\right.\\
&+[\tfrac{1}{2}(\gamma-1)(\gamma P_0)^{-1}]^2\frac{\bar{\lambda}_T}{\bar{\lambda}_u^3}s_w P_1\frac{\mathrm{d}}{\mathrm{d}\xi}\ln P_0\left(\ln\epsilon+\ln\frac{\eta}{\epsilon}\right)\\
&+\frac{\epsilon}{s_w^{\omega}}\tfrac{1}{2}(\gamma-1)(\gamma P_0)^{-1}P_1\left[2s_w+(1-\omega)\left(\frac{\bar{\lambda}_T}{\bar{\lambda}_u}\right)^2-2s_w Pr\right]\\
&\left.+\frac{\epsilon}{s_w^{\omega}}\bar{\lambda}_T s_w^{1-\omega}A_p\right\}. \qquad (2.37a)
\end{aligned}$$

Note that terms proportional to D_1/η in (2.33) and (2.34) have been cancelled by corresponding behaviour from the last term in (2.36), as $\eta \to 0$. The foregoing results confirm the lower-deck thickness in η anticipated, i.e. $\eta = O(\epsilon)$, the proper velocity and temperature scales assumed for the lower deck, as well as the need for the requirement $\epsilon \ll s_w^{\omega}$. The matching of these with the corresponding quantities in the lower deck must obviously be carried out later in the range $\epsilon \ll \eta \ll 1$. The question remains if, indeed, the requirements

$$\frac{\epsilon_p}{s_w} \ll \frac{\epsilon}{s_w^{\omega}} \ll 1 \qquad (2.37b)$$

can be satisfied. These inequalities are suggested by $\epsilon_p \ll \epsilon \ll 1$ in Stewartson's (1974) theory originally developed for $s_w \neq 0$. They will be affirmatively answered later.

2.3. *The lower deck*

The basic solution $U_0(\eta)$, etc. on which the perturbation analysis in the main deck was performed is for the global boundary layer. The slope and coordinate changes of the body surface admissible to the lower deck are so slight that the coordinates used in the main-deck analysis are virtually Cartesian (see figure 2). A difference from this local Cartesian (such as x and y) must, however, be taken into account in the analysis of the lower deck if boundary-layer coordinates (such as x' and y') or their equivalent are to be used, especially if $y_w(x)$ is comparable to the lower-deck thickness of ϵ. The difference in question is $y-y' = y_w(x)$. Note that we have used the normalization for y and y' indicated at the beginning of §2. In changing the Dorodnitsyn variable η for the main deck to the corresponding variable in the lower deck, we observe that for small η

$$\eta = A_0 \int_0 \bar{\rho}\, \mathrm{d}y \sim A_0 \bar{\rho}(0)(y' + y_w). \tag{2.38}$$

Therefore, with (2.1) and (2.6), we can define the reduced lower-deck variables for y' and y_w according to

$$(\tilde{y}, \tilde{y}_w) \equiv \frac{2}{\gamma-1} M_1^{-2} s_w^{-1} (\epsilon_0 M_1)^{-1} \left(\frac{Re}{\gamma C_0}\right)^{\frac{1}{2}} \epsilon^{-1}(y', y_w), \tag{2.39}$$

with which (2.38) furnishes the relation needed:

$$\frac{\eta}{\epsilon} \sim \tilde{y} + \tilde{y}_w. \tag{2.40}$$

In the reduced variables $\tilde{x} = \xi'$, $\tilde{y} = (\eta - \epsilon \tilde{y}_w)/\epsilon$, and the reduced dependent variables for the lower deck inferred from (2.36) and (2.37a),

$$\tilde{u} \equiv \frac{\bar{U}}{\epsilon \lambda_u}, \quad \tilde{v} \equiv \frac{\bar{V}}{\epsilon^2 \Delta^{-1} \lambda_u}, \tag{2.41}$$

$$\tilde{T} \equiv \frac{\bar{T}}{s_w} = 1 + \epsilon \frac{\lambda_T}{s_w} \tilde{T}_1, \tag{2.42}$$

the PDE's governing the lower deck to the leading order for $\tilde{u}$, $\tilde{v}$ and $\tilde{T}_1$ may be reduced to a canonical form, subject to errors of the order ϵ/s_w^{ω},

$$\frac{\partial \tilde{u}}{\partial \tilde{x}} + \frac{\partial \tilde{v}}{\partial \tilde{y}} = 0, \tag{2.43}$$

$$\left(\tilde{u}\frac{\partial}{\partial \tilde{x}} + \tilde{v}\frac{\partial}{\partial \tilde{y}}\right)\tilde{u} + \frac{\mathrm{d}}{\mathrm{d}\tilde{x}} P_1 = \frac{\partial^2 \tilde{u}}{\partial y^2}, \tag{2.44}$$

$$\left(\tilde{u}\frac{\partial}{\partial \tilde{x}} + \tilde{v}\frac{\partial}{\partial \tilde{y}}\right)\tilde{T}_1 = \frac{1}{Pr}\frac{\partial^2}{\partial \tilde{y}^2}\tilde{T}_1, \tag{2.45}$$

after setting

$$P_0 \frac{s_w^{\omega-1}}{\lambda_u} \frac{\Delta}{\epsilon^3} = 1, \tag{2.46}$$

$$\frac{s_w \epsilon_p}{\lambda_u^2 \epsilon^2} \frac{\gamma-1}{2\gamma P_0} = 1, \tag{2.47}$$

where, to be sure, $\lambda_u = s_w^{1-\omega}\bar{\lambda}_u$ and $\lambda_T = s_w^{1-\omega}\bar{\lambda}_T$. These furnish two relations among the three scale factors ϵ, ϵ_p and Δ. Note that, with the exception of an unknown pressure gradient, (2.43)–(2.45) are the same as those for an incompressible boundary layer. The momentum and continuity equations are decoupled from (2.45) and the temperature profile and heat-transfer rate can be computed after solving (2.43) and (2.44). The arrival of the incompressible form, (2.43)–(2.45), should not be too surprising, since temperature and pressure, hence the density, are uniform in the lower deck to the leading approximation.

The main-deck solutions in the inner limit, (2.36) and (2.37*a*), are more than sufficient for providing the outer boundary conditions for the PDE's (2.43)–(2.45) under a small ϵ/s_w^{ω}. Namely, as $\tilde{y} \to \infty$

$$\tilde{u} - \tilde{y} \sim A + \tilde{y}_w, \quad \tilde{T}_1 - \tilde{y} \sim A + \tilde{y}_w. \tag{2.48}$$

These, with (2.46) and (2.47), will assure the matching with the main-deck results in a common domain $\epsilon \ll \eta \ll 1$, or $1 \ll \tilde{y} \ll \epsilon^{-1}$, subject to later confirmation of $\epsilon_p \ll s_w^{1-\omega}\epsilon$ required by (2.37*b*).

The non-slip wall boundary conditions are

$$\tilde{u} = \tilde{v} = \tilde{T}_1 = 0 \quad \text{at} \quad \tilde{y} = 0. \tag{2.49}$$

Far up- and downstream, we require

$$A \to 0 \quad \text{as} \quad \tilde{x} \to -\infty, \tag{2.50}$$

$$A \to -\tilde{y}_w \quad \text{as} \quad \tilde{x} \to +\infty. \tag{2.51}$$

The last requirement follows from the stipulation that the velocity profile will finally merge with that in the downstream global boundary layer which is only slightly perturbed from the state at $\xi = \xi_0$, and therefore $\tilde{u} \sim \tilde{y}$.

2.4. *The pressure–displacement relation*

The function $A(\xi')$ is seen from (2.48) to be indeed a main-deck displacement caused by the presence of the lower deck. One more relation linking $A(\xi')$ to the self-induced pressure $P_1(\xi)$ is required to close the lower-deck system (2.43)–(2.51), which may also furnish the additional condition for completely determining ϵ, ϵ_p and Δ in terms of s_w, Re and M_1. It is essential to observe that $P_1(\xi')$ cannot be directly related to $A'(\xi')$, as it was in the classical theory, since it is the displacement of the main deck's outer edge (not that of the lower deck) that determines the change in pressure $P_1(\xi')$, and that the latter will be affected by certain higher-order terms which prove to be of first-order importance at low wall temperature.

The P_1–A relation should follow from a thorough analysis of the upper deck and its matching with the main deck. The relation sought may also be obtained through the displacement thickness δ^* of the main deck; this appears to be particularly simple for a hypersonic boundary layer which has a sharp outer edge, i.e. $\delta \approx \delta^*$ (Stewartson 1955; Hayes & Probstein 1959; Moore 1964). Let us calculate δ^* in the hypersonic limit

$$\delta^* = \delta \int_0^\infty \left(1 - \frac{\rho u}{\rho_e u_e}\right) \mathrm{d}y = \frac{\gamma - 1}{2\gamma} \frac{\delta}{\epsilon_0^2 A_0} \frac{1}{\bar{p}} \int_0^\infty \left(\bar{T} - \frac{\bar{T}_e}{\bar{U}_e}\bar{U}\right) \mathrm{d}\eta$$

or

$$\frac{M_1 \delta^*}{L} = \tfrac{1}{2}(\gamma - 1)\,\gamma^{\frac{1}{2}}(\epsilon_0 M_1)^{-3}\chi_0 \frac{\displaystyle\int_0^\infty (\bar{T} - \bar{T}_e \bar{U}/\bar{U}_e)\,\mathrm{d}\eta}{[1 + \gamma(M_1\epsilon_0)^{-2}\epsilon_p P_1 + \ldots]}, \tag{2.52}$$

where χ_0 is the hypersonic interaction parameter†

$$\chi_0 \equiv M_1^3\left(\frac{C_0}{Re}\right)^{\frac{1}{2}}, \tag{2.53}$$

and we have used $p/p_e = 1$ and $P_0 = (1/\gamma)(M_1\epsilon_0)^2$ in approximating $\bar{p}$ in (2.52). In (2.52), the integration ranges from the wall up to the main-deck outer edge, which includes the lower deck. The contribution to the integral comes principally from the main-deck solutions; the latter leads, however, to a non-integrable singularity in the lower limit, owing to the solution behaviour (2.37*a*). To resolve this ambiguity, we introduce an indefinite integral

$$I(\eta;\xi') \equiv \int_0 [\bar{T}-(\bar{T}/\bar{U})_e\,\bar{U}]\,\mathrm{d}\eta \tag{2.54}$$

so that the integral in question is the limit $I(\infty;\xi')$ and that $\partial I/\partial\eta = \bar{T}-(\bar{T}/\bar{U})_e\,\bar{U}$. In the main deck ($0 < \eta < \infty$), I can be evaluated as

$$I = I(\infty;\xi') + \int_\infty [\bar{T}-(\bar{T}/\bar{U})_e\,U]\,\mathrm{d}\eta \tag{2.55}$$

with the integrand of the second integral computed from the main-deck solution, whereas in the lower deck I is evaluated with its integrand determined by the lower-deck analysis. The contribution of $(\bar{T}/\bar{U})_e\,\bar{U}$ to the integrand of (2.54) and (2.55) belongs to an order higher than that of $\bar{T}$ for a boundary-layer approximation with a hypersonic outer flow, and is negligible as M_1^{-2} in the present study (Stewartson 1955; Moore 1964).

With the omission of $(\bar{T}/\bar{U})_e\,\bar{U}$ from (2.55) and the main-deck solution $\bar{T}$, the main-deck result of I in the inner limit ($\eta \to 0$) may be obtained as

$$\begin{aligned} I(\eta;\xi') \sim{}& I(\infty;\xi') - \int_0^\infty T_0(\eta)\,\mathrm{d}\eta + \epsilon s_w A(\xi') \\ & - \epsilon_p \int_0^\infty [T_p - \tfrac{1}{2}(\gamma-1)P_1 s_w^{1-\omega}\bar{\lambda}_T(D_1\eta^{-1} - D_2\ln\eta)(1+\eta)^{-2}]\,\mathrm{d}\eta \\ & + \epsilon_p \tfrac{1}{2}(\gamma-1)P_1 s_w^{1-\omega}\bar{\lambda}_T\left[D_1\ln\eta - D_2\eta(\ln\eta - 1)\right. \\ & \left. - \mathrm{FP}\,D_1\int_0^\infty \frac{\mathrm{d}\eta}{(1+\eta)^2\eta} + D_2\int_0^\infty \frac{\ln\eta}{(1+\eta)^2}\,\mathrm{d}\eta\right] \\ & + s_w\eta + s_w^{1-\omega}\bar{\lambda}_T(\tfrac{1}{2}\eta^2 + \epsilon A\eta), \end{aligned} \tag{2.56}$$

where FP signifies the finite parts of the integrals

$$\lim_{\eta\to 0}\left[\int_\eta^\infty \frac{\mathrm{d}\eta}{(1+\eta)^2\eta} + \ln\eta\right]$$

† Note that if a linear viscosity–temperature model is used, C_0 will be replaced by C of (2.14), and χ_0 is identified with the interaction parameter $\chi \equiv M_1^3(C/Re)^{\frac{1}{2}}$ (Hayes & Probstein 1959; Moore 1964).

and T_0 is the leading-order expansion of $\bar{T}$, not to be confused with the stagnation temperature. In the above, we have introduced terms with the factor $(1+\eta)^{-2}$ in the integrand with corresponding terms added to I in order to render the resulting integrand integrable in both limits 0 and ∞ without altering the correct behaviour of T_p and I in the inner limit. In the lower-deck ($0 < \tilde{y} \ll \epsilon^{-1}$), in terms of the lower-deck variables, I can be computed as

$$I = s_w \epsilon \int_0 [1 + \epsilon s_w^{-\omega} \bar{\lambda}_T \tilde{T}_1 + \ldots] \, d\tilde{y}$$

$$= s_w \epsilon \tilde{y} + \epsilon^2 s_w^{1-\omega} \bar{\lambda}_T \int_0 (\tilde{T}_1 - \tilde{y} - A - \tilde{y}_w) \, d\tilde{y} + \epsilon^2 s_w^{1-\omega} \bar{\lambda}_T [\tfrac{1}{2}\tilde{y}^2 + (A - \tilde{y}_w)\tilde{y}] + \ldots. \tag{2.57a}$$

Matching of the main-deck and lower-deck results for $I(\eta; \xi')$ in the range (recall $\eta \sim \epsilon(\tilde{y} + \tilde{y}_w)$)

$$\epsilon \ll \eta \ll 1 \quad \text{or} \quad 1 \ll \tilde{y} \ll \epsilon^{-1} \tag{2.57b}$$

establishes that

$$I(\infty, \xi') = \int_0^\infty T_0(\eta) \, d\eta$$

$$- \epsilon s_w \left\{ A - \left(\frac{\epsilon_p}{\epsilon s_w} \right) \int_0^\infty \left[T_p - \tfrac{1}{2}(\gamma - 1) P_1 s_w^{1-\omega} \bar{\lambda}_T \frac{D_1/\eta - D_2 \ln \eta}{(1+\eta)^2} \right] d\eta \right\} + \ldots, \tag{2.58}$$

where ... are the unmatched remainder of the two expansions dominated by

$$\epsilon_p \tfrac{1}{2}(\gamma - 1) P_1 \bar{\lambda}_T s_w^{1-\omega} [D_1(1 + \ln \eta) - D_2 \eta (\ln \eta - 1)] + \ldots$$

from the main-deck solution. This, taking into consideration the dependence of D_1 and D_2 on s_w, (2.35*b*, *c*), is seen to be at most of order $\epsilon_p s_w^\omega \ln \eta$, $\epsilon_p \eta$ and $\epsilon^2 s_w^{1-\omega}$, being much smaller than terms of order ϵs_w and ϵ_p retained under the inequality (2.37*b*) and for the range of η, (2.57*b*), considered. Note that the products $s_w^{1-\omega} D_1$ and $s_w^{1-\omega} D_2$ in the integrand of (2.58) are of orders s_w^ω and $s_w^{1+\omega}$, respectively. It is also essential to point out that the second term inside the square brackets of (2.58) does not represent a higher-order correction to T_p comparable with $s_w^{1-\omega} D_1$ and $s_w^{1-\omega} D_2$; it serves only to cancel the corresponding singularities in T_p in the limit $\eta \to 0$. In passing, we note that the terms of order $\epsilon s_w^\omega \ln \eta$ in the remainder would be matched by corresponding terms from the lower-deck solution pertaining to the next order, which is not needed, however, in the approximation level considered.

It is thus seen that the main-deck displacement thickness δ^* is unaffected by the lower deck up to the order ϵs_w, so long as $\epsilon_p / \epsilon s_w$ is bounded and ϵ / s_w^ω is small; the latter provision will be substantiated later. The result is valid for a small as well as a unit-order s_w. In the latter case, the second right-hand member of (2.58) becomes simply $-\epsilon s_w A$.

We can now apply (2.58) to (2.52) under the hypersonic outer-edge condition and for a small χ. In this case we should take $\epsilon_0 = M_1^{-1}$ and then use the Prandtl–Glauert formula allowed by the upper deck

$$(p_e - p_1)/p_1 = \gamma M_1^2 (M_1^2 - 1)^{-\frac{1}{2}} (L)^{-1} \, d\delta^*/dx,$$

yielding

$$P_1 = -\gamma^{\frac{1}{2}}(\gamma-1)\frac{\epsilon s_w}{\epsilon_p \Delta}\chi_0\left\{\frac{dA}{d\xi'}+\gamma\left(\frac{\epsilon_p}{\epsilon s_w}\right)\frac{dP_1}{d\xi'}\int_0^\infty T_0(\eta)\,d\eta\right.$$
$$\left.-\frac{\epsilon_p}{\epsilon s_w}\int_0^\infty\left[\frac{\partial}{\partial\xi'}(T_p)-\tfrac{1}{2}(\gamma-1)\bar{\lambda}_T s_w^{1-\omega}\frac{dP_1}{d\xi'}\frac{D_1/\eta-D_2\ln\eta}{(1+\eta)^2}\right]d\eta\right\}. \quad (2.59)$$

Using (2.35a) for T_p, we arrive at a P_1–A relation

$$P_1 = -\sigma\frac{d}{d\xi'}(A+\nu P_1), \quad (2.60)$$

where

$$\sigma \equiv \gamma^{\frac{1}{2}}(\gamma-1)\frac{\epsilon s_w}{\Delta\epsilon_p}\chi_0, \quad (2.61)$$

$$\nu \equiv k\epsilon_p/\epsilon s_w \quad (2.62)$$

and

$$k \equiv \int_0^\infty T_0(\eta)\,d\eta-\tfrac{1}{2}(\gamma-1)\left[\int_0^\infty T_0(T_0 U_0^{-2}-D_1\eta^{-2}-D_2\eta^{-1})\,d\eta\right.$$
$$\left.+\int_0^\infty(D_1\eta^{-1}-D_2\ln\eta)\left(T_0'-\frac{s_w^{1-\omega}\bar{\lambda}_T}{(1+\eta)^2}\right)d\eta\right]. \quad (2.63)$$

With (2.60) the lower-deck problem, (2.43)–(2.45) and (2.48)–(2.51), can be considered closed; they may be compared to the corresponding equations in the classical triple-deck theory. Equations (2.46) and (2.47) with (2.61) and (2.62) furnish four relations for the five parameters ϵ, ϵ_p, Δ, ν and σ. The single degree of freedom left can be used to make the final system and its successive development more well-ordered; this will bring out clearly the existence of a characteristic wall-temperature level and the three distinct wall-temperature ranges. In passing, we point out that for $Pr = 1$ and $\omega = 1$, the value of k can be explicitly evaluated as

$$k = 0.663+1.722s_w-(\gamma-1)(0.367-0.836s_w+0.412s_w^2).$$

2.5. *Three wall-temperature ranges*

Examination of relations (2.46), (2.47), (2.61) and (2.62) and the pressure–displacement law (2.60) indicates a characteristic wall-temperature level

$$s_w^* \equiv [(\bar{\lambda}_u)^5\gamma^{-\frac{1}{2}}k^4[\tfrac{1}{2}(\gamma-1)]^{-2}\chi_0]^{\frac{1}{(4\omega+2)}} \quad (2.64)$$

and the existence of three distinct wall temperature ranges: (i) supercritical, $s_w \gg s_w^*$; (ii) transcritical, $s_w = O(s_w^*)$; and (iii) subcritical, $s_w \ll s_w^*$. For $\chi_0 \ll 1$, a small s_w^* is implicit. These follow from observing from (2.46), (2.47), (2.61) and (2.62) that

$$\nu^4\sigma = (s_w^*/s_w)^{4\omega+2} \quad (2.65)$$

and that

$$\epsilon = k^{-1}(\bar{\lambda}_u)^{-2}\tfrac{1}{2}(\gamma-1)\,s_w^{2\omega}\nu, \quad (2.66)$$

$$\epsilon_p = k^{-2}(\bar{\lambda}_u)^{-2}\tfrac{1}{2}(\gamma-1)\,s_w^{2\omega+1}\nu^2, \quad (2.67)$$

$$\Delta = k^{-3}(\bar{\lambda}_u)^{-5}\gamma[\tfrac{1}{2}(\gamma-1)]^3 s_w^{4\omega+2}\nu^3. \quad (2.68)$$

For $s_w \gg s_w^*$ (supercritical), we shall set $\sigma = 1$; therefore

$$\nu = (s_w^*/s_w)^{\omega+\frac{1}{2}} \ll 1 \quad (2.69)$$

and smallness of ϵ, ϵ_p and Δ is assured. It also follows from (2.64) and (2.66) that ϵ is gauged by $(\gamma-1)^{\frac{1}{2}}s_w^{\omega-\frac{1}{2}}\chi_0^{\frac{1}{2}}$. In this case, (2.60) becomes

$$P_1 = -\frac{\mathrm{d}}{\mathrm{d}\xi'}(A+\nu P_1), \tag{2.70}$$

where ν given by (2.69) obviously gauges the departure from the classical theory (cf. Stewartson 1974, 1981; Stewartson & Williams 1969, 1973; Messiter 1979; Neiland 1969, 1971; Sychev 1974, 1987; and Smith 1982, 1989). For $s_w = O(s_w^*)$, i.e. the transcritical range, we have $\nu = O(1)$, and the parameters in (2.66)–(2.68) remain small since s_w is necessarily small; hence we can still set $\sigma = 1$. But the lower-deck problem with a unit-order σ and ν in (2.60) can no longer represent a small departure from the classical theory. Beyond this range with a much lower s_w, the scales based on $\sigma = 1$ are not the proper set, since ν would become unbounded and the expansions are not well-ordered. For the subcritical range, $s_w \ll s_w^*$, we therefore set instead $\nu = 1$, which assures ϵ, ϵ_p and Δ in (2.66), (2.67) and (2.68) to be small, and (2.65) gives

$$\sigma = (s_w^*/s_w)^{4\omega+2} \gg 1, \tag{2.71}$$

and the pressure–displacement law assumes a non-degenerate form

$$\frac{\mathrm{d}}{\mathrm{d}\xi'}(P_1+A) = -\sigma^{-1}P_1. \tag{2.72}$$

This yields a relation fundamentally different from the classical law $P_1 = -\mathrm{d}A/\mathrm{d}\xi'$; moreover, according to (2.66)–(2.68), the ϵ and Δ gauging the relative scale of the triple deck, as well as the ϵ_p gauging the induced pressure, become independent of χ_0 or Re and M_1, being determined principally by the wall-temperature ratio s_w. The system with $\nu = 1$ obviously overlaps that with $\sigma = 1$ in the transcritical range.

The requirements on the smallness of ϵ_p/s_w and ϵ/s_w^ω made earlier in (2.37*b*) are readily verified from (2.66) and (2.67). Two additional parametric assumptions corresponding to the neglect of the centrifugal force effect on the main-deck pressure ($\epsilon_p' \ll \epsilon_p$) and of the nonlinear correction ($\epsilon^2 \ll \epsilon_p$) also follow. From (2.66)–(2.28), one can establish that

$$\frac{\epsilon_p'}{\epsilon_p} = \frac{\nu\sigma^2}{k_2^{\frac{1}{2}}(\gamma-1)M_1^2 s_w}, \tag{2.73}$$

$$\frac{\epsilon^2}{\epsilon_p} = (\bar{\lambda}_u)^{-2}2^{\frac{1}{2}}(\gamma-1)\,s_w^{2\omega-1}. \tag{2.74}$$

Therefore to neglect the pressure variation across the main deck, one needs a sufficiently high outer-edge Mach number and a not so low wall temperature, i.e. a sufficiently low T_1/T_w. According to (2.74), the nonlinear effects gauged by ϵ^2 can be neglected if the viscosity–temperature relation obeys $\omega > \frac{1}{2}$, but must be taken into account fully if $\omega = \frac{1}{2}$ for a cold wall.

As noted earlier, the significant influence of the wall temperature is a consequence of a very special form of the perturbation-temperature profile (2.29), which affects the displacement thickness in direct proportion to s_w (see (2.56), (2.58) or (2.59)). This enhances the relative importance of pressure changes on the main-deck displacement at low wall temperature and explains the presence of $\mathrm{d}P_1/\mathrm{d}\xi'$ in (2.70) and (2.72). The reduced lower-deck equations with either (2.70) or (2.72) are identical to those of the

Newtonian theory (Brown *et al.* 1975) even though γ is not taken to be near unity here and s_w was not assumed to be low there. This coincidence should not be too surprising, if one realizes that the perturbation pressure therein was amplified by a large χ, enhancing therefore its relative importance to the main-deck displacement without the need to reduce s_w. The differences of the present analysis from Brown *et al.* (1975) could be viewed as consequences of trading the requirement of a small χ with that of a small $(\gamma-1)$. In addition to relaxing the restriction on the specific-heat ratio, a critical analysis on the influence of the viscosity–temperature law on triple-deck structure at low s_w has been made. Of theoretical interest here is of course the identification of a characteristic s_w determined by χ_0 and the three distinct domains that follow. One surmises that a characteristic value of $\gamma \neq 1$ with three distinct Newtonian domains that follow could also be identified in Brown *et al.* (1975) for the Newtonian model.

An interesting analogy between a shallow liquid layer flowing down a slope and the Newtonian triple-deck problem (Brown *et al.* 1975) in the limit $\chi \to \infty$ has been noted by Gajjar & Smith (1983), corresponding to an infinite σ in (2.72), and hence $P_1 + A = 0$. The compressive free-interaction problem was solved therein with $P_1 = -A$, which exhibits a power-law growth in ξ' far downstream. For a large but finite σ, however, (2.72) indicates the admission of a plateau value at large ξ', which will be determined in the computational study in §3.

3. Computational study: compressive free interaction and ramp-induced separation/interaction

Existing numerical results for the lower-deck problem at lower Mach numbers, particularly those from Stewartson (1974, 1981), Stewartson & Williams (1969), Smith (1982, 1986), Brown *et al.* (1975), Rizzetta *et al.* (1978), Jenson (1977) and Gajjar & Smith (1983), can be compared with the present computational study, since they share the same reduced equation system, except for the need to identify the proper values for the parameter ν in (2.70) or σ in (2.72). The available data are far from adequate, however, in ascertaining and distinguishing the solution features related to the wall-cooling effect. As examples of laminar separation in hypersonic boundary layers, we shall discuss computational studies for two problems: (*a*) compressive free interaction, (*b*) ramp-induced interaction. The former may be regarded as caused by the presence of an incident shock or a ramp of sufficient strength far downstream of the triple deck. Detail comparison with existing triple-deck results as well as data generated by the iterative boundary-layer method will be made, after a brief description of the key features in the computation algorithm and the method of its implementation.

3.1. *Numerical procedure*

We solve the discretized form of the lower-deck equation system, (2.43), (2.44), (2.48)–(2.51) with the pressure–displacement relation (2.70) or (2.72), using the primitive variables u, v and p. For convenience, the tildes over the lower-deck variables will henceforth be omitted and x will be written for ξ'. Central differences are used throughout to retain second-order accuracy. For the compressive free-interaction problem, a second-order-accurate, implicit marching scheme employing a large-band matrix solver (LINPACK) is used. In the reverse-flow region, the Flügge–Lotz and Reyhner (FLARE) model is adopted, following Stewartson (1974, 1981) and Stewartson & Williams (1969). That is, the program will delete $u\,\partial u/\partial x$

wherever $u < 0$. A mesh, uniform in the x-direction ($\Delta x = 0.10$) and increasing progressively in the y-direction from $\Delta y = 0.02$, was used.

For the ramp problem, a relaxation procedure utilizing again a large-band direct solver for the entire domain is developed and the nonlinear, coupled equations are solved in an implicit manner. The nonlinear terms are linearized by Newton's method. Denoting the iteration stage by n, $u^{n+1}-u^n$ by Δu, and the central x-difference quotient by δ_x, the implicit relaxation scheme treats uu_x, for example, as

$$\begin{aligned} uu_x &= u^{n+1}u_x^{n+1} \\ &= u^n u_x^n + (u^n\delta_x + u_x^n)\,\Delta u + O(\Delta u)^2. \end{aligned} \tag{3.1}$$

A smoothly varying grid with total grid points comparable to (30×15) for Grid 1, or (60×30) for Grid 2, is used. Convergence with residue reducing down to 10^{-4} was achieved typically in seven iterations for Grid 1, and fifteen for Grid 2 on a UNIX 3-260. The convergence with respect to mesh size and the adequacy of the grid will be examined later. The FLARE model for the reverse-flow region has been used only in the free-interaction problem.

The upstream and downstream conditions (2.50) and (2.51) are implemented with partial differential relations equivalent to the asymptotic expansions for large $|x|$ upstream (Lighthill 1953; Stewartson 1974, 1981; Stewartson & Williams 1969; Smith 1982) and downstream (Smith & Stewartson 1973)

$$\frac{\partial u}{\partial x} \sim k(u-y), \quad x \to -\infty, \tag{3.2}$$

$$\frac{\partial u}{\partial x} \sim \frac{2y}{3x} - \left(u + y\frac{\partial u}{\partial y}\right)\Big/ 3x, \quad x \to \infty \tag{3.3}$$

where k satisfies $1 + \sigma\nu k = 1.2879\sigma k^{\frac{4}{3}}$. In the free-interaction problem, (3.3) will not be applied, and Lighthill's (1953) type of linear solutions are used as initial conditions.

3.2. *Compressive free interaction*

Compressive free-interaction solutions to (2.43), (2.44), (2.48)–(2.51) with $y_w \equiv 0$ have been generated in the σ and ν ranges corresponding to all three wall-temperature domains. The special case $\sigma = 1$, $\nu = 0$, affords a detail comparison with the well-established result of Stewartson & Williams (1973). At separation, for example, the present program gives 1.0261 as compared to 1.0260 from Stewartson & Williams (1973). The plateau value of P reached by the present program in this case is 1.809, which is closed to the 1.80 inferred in Stewartson (1974, 1981) and Smith (1982) and from other sources. The value 1.809 is, in fact, not far from the value arrived at in Williams' more definitive work (Williams 1975) which resolves the ambiguity of the FLARE model with more thorough treatment of the reversed-flow region.

Figure 3 presents the pressure p as a function of x for $\nu = 1$ and $\sigma = 1$, 2, 10, 50 and ∞. The case with $\sigma = \nu = 1$, typical of the transcritical wall-temperature range can be compared with corresponding results from the Newtonian theory (Brown *et al.* 1975). At the point of zero wall shear ($x = 0$), the present data give $P = 0.811$, being close to the 0.810 given by Brown *et al.* (1975). The latter work did not reach a plateau pressure, which is $P = 1.681$ according to the present work. For the case of $\sigma = 1$, $\nu = 2$, corresponding to $\sigma = 2$ in Brown *et al.*'s (1975) notation, the present program gives $P = 0.581$ at separation, compared to 0.588 from Brown *et al.* (1975).

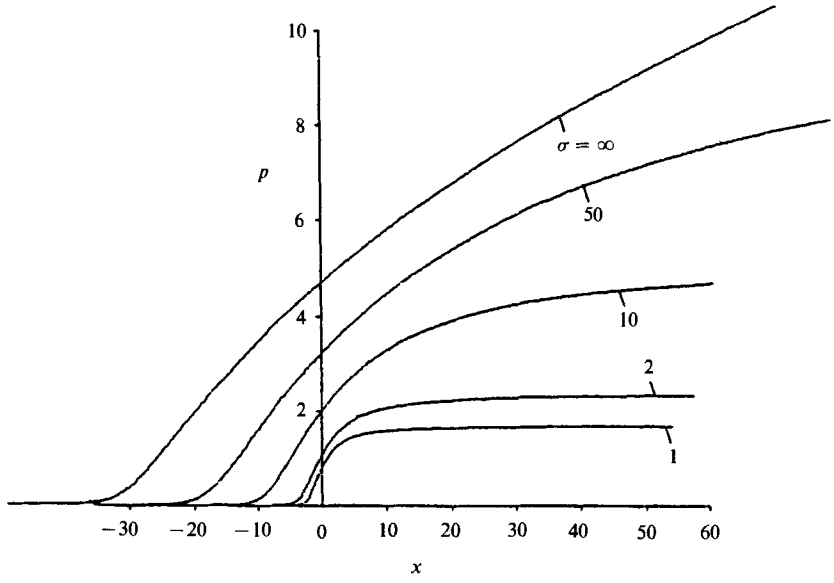

FIGURE 3. Comparison of over-pressures in a free interaction at different levels of wall temperature corresponding to $\sigma = 1, 2, 10, 50$ and ∞. The over-pressures at $x = 0$ (separation point) are 0.811, 1.088, 2.018, 3.234 and 4.712 for $\sigma = 1, 2, 10, 50$ and ∞, respectively. The plateau pressures are 1.681, 2.340 and 4.960 for $\sigma = 1, 2$ and 10, respectively. Note, the variable ξ' (cf. (2.24)) is written for expediency as x.

The plateau pressure is $P = 1.564$ in this case. Figure 3 indicates that the value of $\sigma = 50$ is still far from the limit $\sigma \to \infty$. The solution in the limit $\sigma \to \infty$ compares closely with that given earlier by Gajjar & Smith (1983). The corresponding wall-shear distribution and velocity profiles at successive x-stations in this case are documented in Brown *et al.* (1989).

3.3. *Ramp-induced interaction*

We considered next the generic problem of an inviscid–viscous interaction induced by a sharp-corner ramp

$$\begin{aligned} y &= 0 \quad \text{for} \quad x < 0, \\ &= \alpha x \quad \text{for} \quad x > 0, \end{aligned} \tag{3.4}$$

where x and y are in lower-deck variables and the physical ramp angle α^* is normalized as

$$\alpha \equiv \alpha^* / \gamma^{\frac{1}{2}} (\gamma - 1) A^{-1} M_1^{-1} \epsilon s_w \chi_0. \tag{3.5}$$

In this case a relaxation scheme is used in the solution method. A unique feature with the sharp-corner solution in boundary-layer-type coordinates is a discontinuity in the x-derivative of the lower-deck solution at $x = 0$ for all y. It can be shown that, at $x = 0$, the pressure gradient is continuous, but

$$\left[\frac{\partial u}{\partial x}\right] = \alpha \frac{\partial u}{\partial y}, \quad \left[\frac{\partial v}{\partial x}\right] = -2\alpha \left\langle \frac{\partial u}{\partial x} \right\rangle \tag{3.6}$$

where the symbols [ ] and $\langle\ \rangle$ signify the difference and the arithmetic mean of downstream and upstream values, respectively. These jump conditions, together with the continuity of $\partial p/\partial x$ are used in the program, and prove to be helpful in

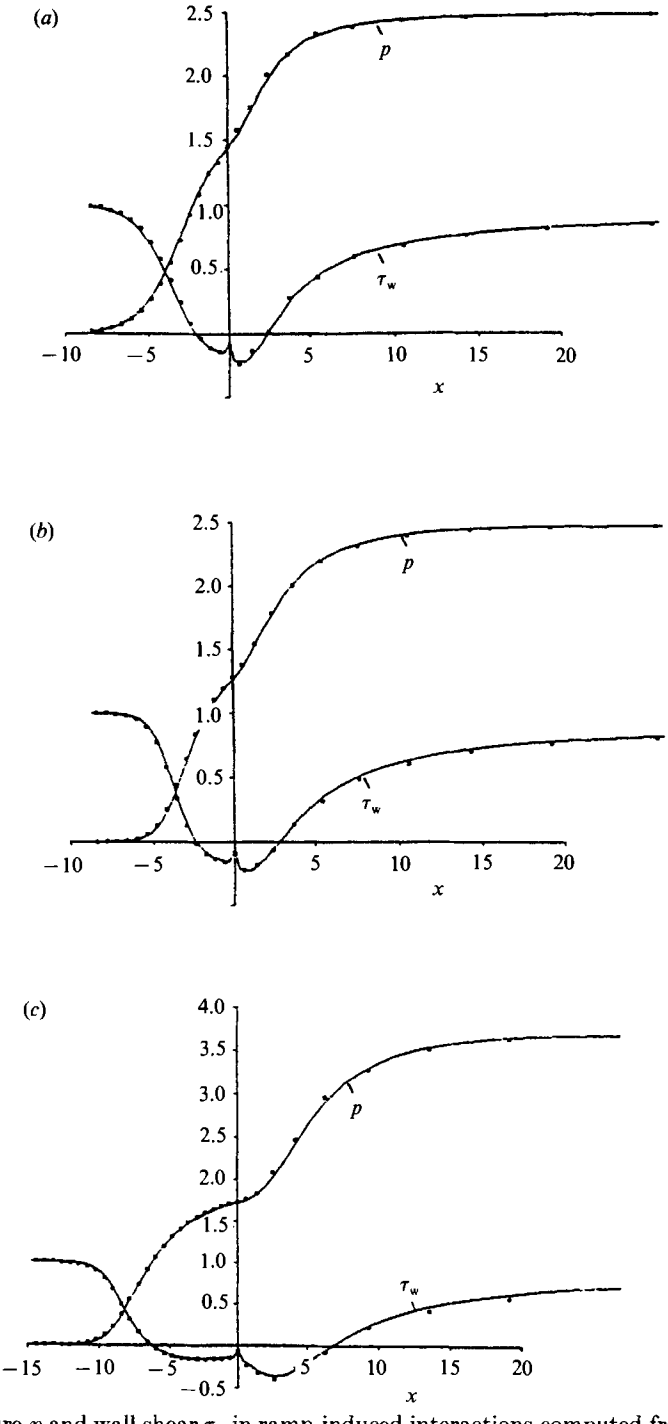

FIGURE 4. Over-pressure p and wall shear τ_w in ramp-induced interactions computed from two sets of grids at a reduced ramp angle $\alpha = 2.5$: (*a*) a supercritical case ($\nu = 0$, $\sigma = 1$), (*b*) a transcritical case ($\nu = \sigma = 1$), (*c*) another transcritical case ($\sigma = 1.5$, $\nu = 1$). The dots represent the results of coarse-grid calculations, (30×15) for (*a*) and (*b*), and (40×15) for (*c*). The continuous solid curves represent the results of fine-grid calculations, (60×30) for (*a*) and (*b*), and (80×30) for (*c*). Note that (*a*) corresponds to the classical triple-deck theory.

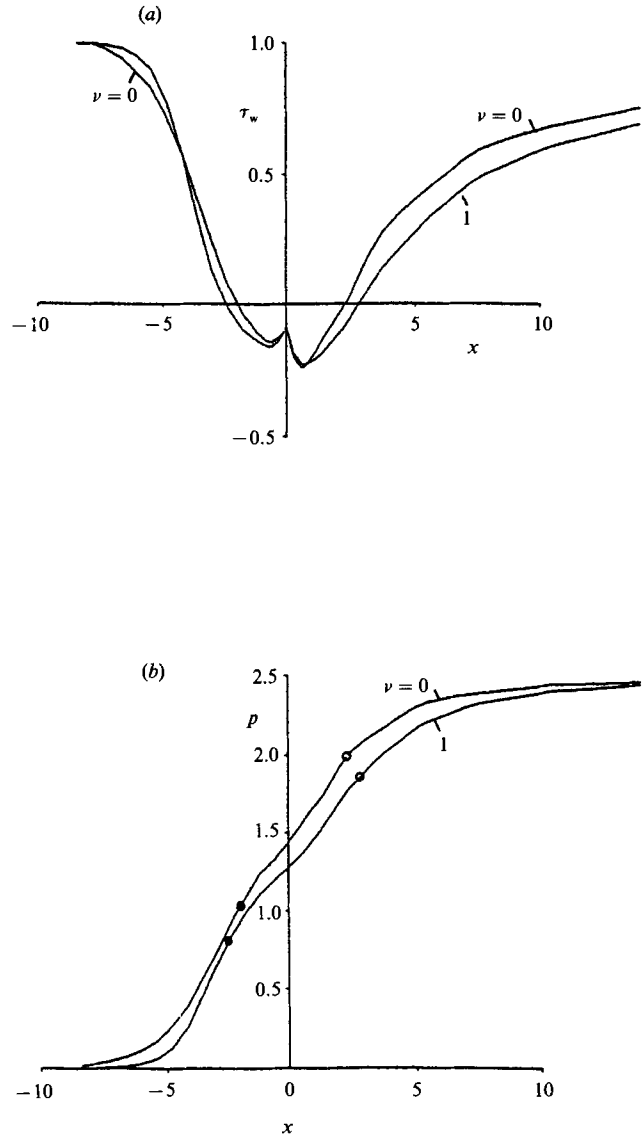

FIGURE 5. (*a*) Ramp-induced wall shear and (*b*) pressure at supercritical and transcritical wall temperatures corresponding to $\sigma = 1$ and $\nu = 0$ and 1 at a reduced ramp angle $\alpha = 2.5$. Note that the filled and open circles denote the separation and reattachment points, respectively.

capturing the solution behaviour next to the corner. Associated with these is a singularity in wall shear at the corner, noted by Stewartson (Stewartson 1974, 1981; Messiter 1979)

$$\frac{\mathrm{d}\tau_w}{\mathrm{d}x} \sim \pm C_s \alpha |x|^{-\frac{1}{3}}, \quad x \to \pm 0, \tag{3.7}$$

respectively, and Jenson's (1977) work establishes that

$$C_s = \pm 0.7866 |\tau_w(0)|^{\frac{4}{3}} \tag{3.8}$$

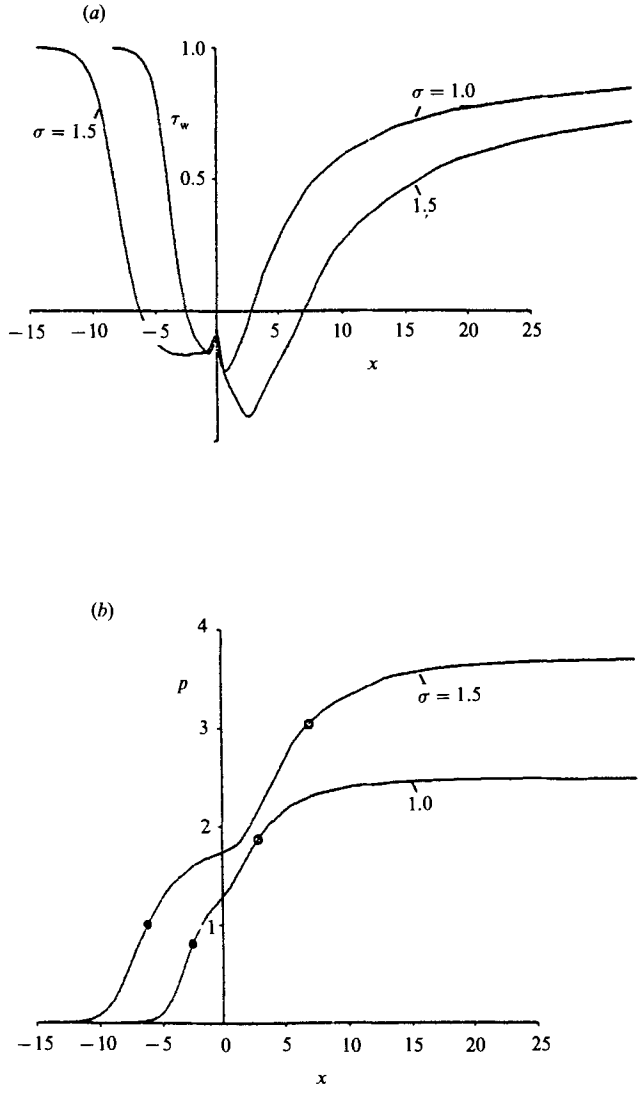

FIGURE 6. (*a*) Ramp-induced wall shear and (*b*) pressure at two transcritical wall temperatures corresponding to $\nu = 1$ and $\sigma = 1$ and 1.5 at a reduced ramp angle $\alpha = 2.5$. Note that the filled and open circles denote the separation and reattachment points, respectively.

in the unseparated case (+) and in the separated case (−). This provides a critical test in the solution accuracy to be studied later.

Before presenting the numerical results and their comparison with existing works, the sensitivity of results on mesh size, and hence the accuracy, will first be examined. For this purpose, two groups of pressure and wall-shear results are presented in figure 4(*a–c*) for $\alpha = 2.5$. The results shown are for $\sigma = 1$, $\nu = 0$; $\sigma = \nu = 1$; and $\sigma = 1.5$, $\nu = 1$, corresponding to a supercritical and two transcritical wall-temperature ranges. Each dot in figure 4(*a–c*) represents the computed value from the coarser grid, and results from calculations using the finer grid are presented as continuous solid curves. Of interest is not only the good agreement of the coarse- and fine-mesh results, but the apparent capability of the coarse mesh to reproduce the solution behaviour about

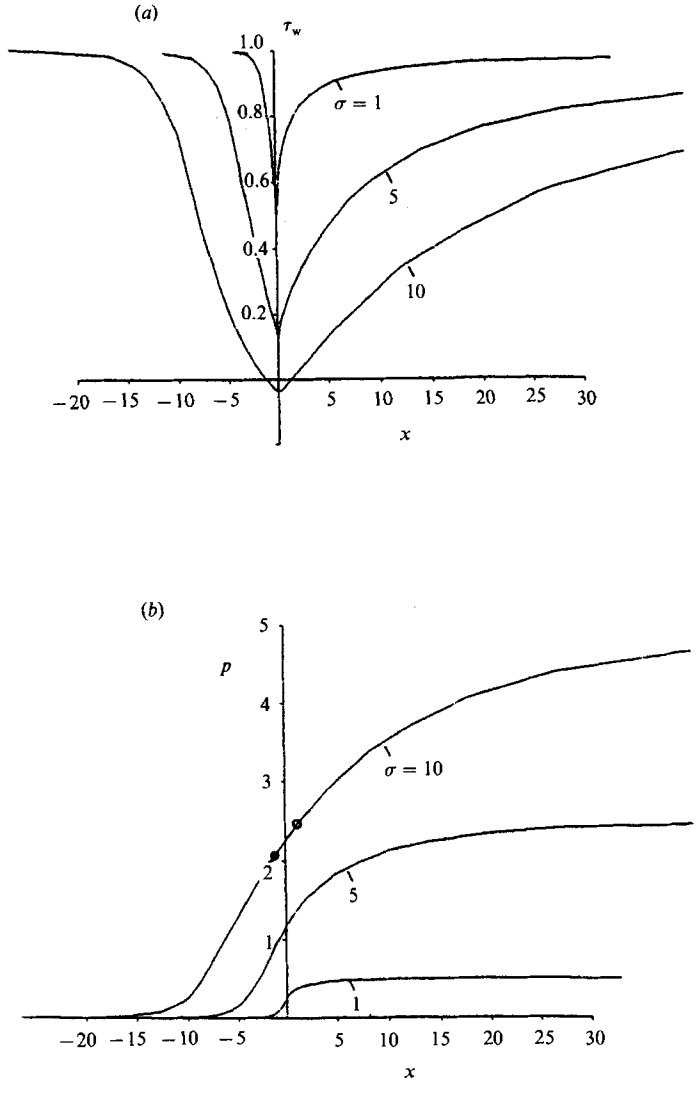

FIGURE 7. (*a*) Ramp-induced wall shear and (*b*) pressure at subcritical wall temperatures corresponding to $\nu = 1$ and $\sigma = 1$, 5 and 10 at a reduced ramp angle $\alpha = 0.5$. Note that the filled and open circles denote the separation and reattachment points.

the corner singularity. Detail comparison of the wall-shear distributions with the analytic result (3.7), (3.8) does support this expectation. Similar results for $\alpha = 1$ and 2 are documented in Brown *et al.* (1989).

In figures 5(*a*) and 5(*b*), we present the wall shear τ_w and pressure P for the super- and transcritical s_w range (thus setting $\sigma = 1$) for reduced ramp angle $\alpha = 2.5$. (Again, see Brown *et al.* 1989 for the cases of $\alpha = 1$ and 2 not shown here.) In the figures results for two different values of ν (0 and 1) signifying different degrees of the transcritical effect are shown. The filled and open circles in figure 5(*b*) denote P-values at separation and reattachment, respectively. Corresponding solutions more pertinent to the transcritical domains are presented in figures 6(*a*) and 6(*b*) for which we set $\nu = 1$ and compare results for $\sigma = 1$ and $\sigma = 1.5$ for $\alpha = 2.5$. Increases

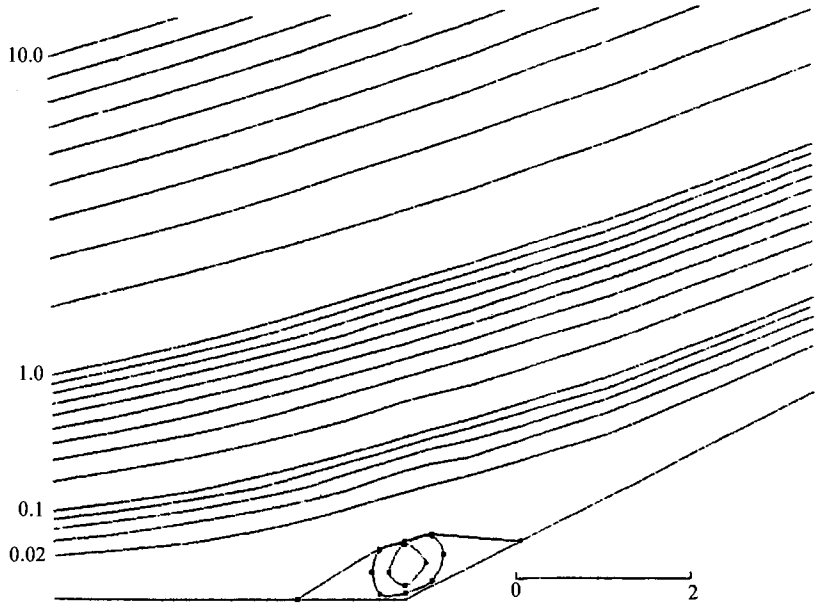

FIGURE 8. Streamline pattern with separation bubble corresponding to figure 7 for $\nu = 1$ and $\sigma = 10$. The contours are drawn in the reduced, lower-deck, boundary-layer coordinates.

in separation-eddy size and plateau pressure in the normalized variables are apparent with the larger σ ($\sigma = 1.5$). To be sure, as $s_w \sim T_w/T_0$ reduces, corresponding to an increasing σ, the extent of the triple deck as well as the amplitude of the induced pressure is expected to diminish rather than becoming large. The manner in which s_w controls the eddy behaviour and the upstream influence needs to be more explicitly expressed and will be examined more precisely shortly.

The calculation has not been as successful for σ beyond 1.5 for the larger ramp angles ($\alpha = 2.5$), for which the convergence becomes problematic, owing largely to the inadequate treatment of the reverse-flow region, it is believed. Use of a FLARE-type remedy, or other differencing and iterative strategies, to enlarge the domain of analysis in σ and α remain to be studied. For smaller ramp angles, however, solutions for subcritical cases with σ as large as 5 for $\alpha = 1$, and 10 for $\alpha = 0.5$ can be obtained. In figures 7 and 9, the wall shear and pressure are presented for $\alpha = 0.5$ and 1. Figures 8 and 10 show the streamline patterns for $\alpha = 0.5$, $\sigma = 10$ and for $\alpha = 1$, $\sigma = 5$, respectively.

3.4. *Comparison with corresponding triple-deck and IBL solutions at lower supersonic Mach numbers*

In the reduced variables it is possible to compare the numerical solutions generated in the present study with corresponding solutions obtained in the earlier triple-deck studies (Rizzetta *et al.* 1978; Jenson 1977) as well as results by interactive boundary-layer (IBL) methods (Werle & Vatsa 1974). Figure 11 reproduces the triple-deck results from Rizzetta *et al.* (1978) and the corresponding solutions from figure 4(*a*) for $\sigma = 1$ and $\nu = 0$ for the reduced ramp angle $\alpha = 2.5$. In view of the good agreement between the present solutions based on two sets of grid, only the coarse-mesh data from figure 4(*a*) are shown (as dots). (See Brown *et al.* 1989 for smaller reduced ramp angle.) The present work predicts a noticeably smaller extent for the

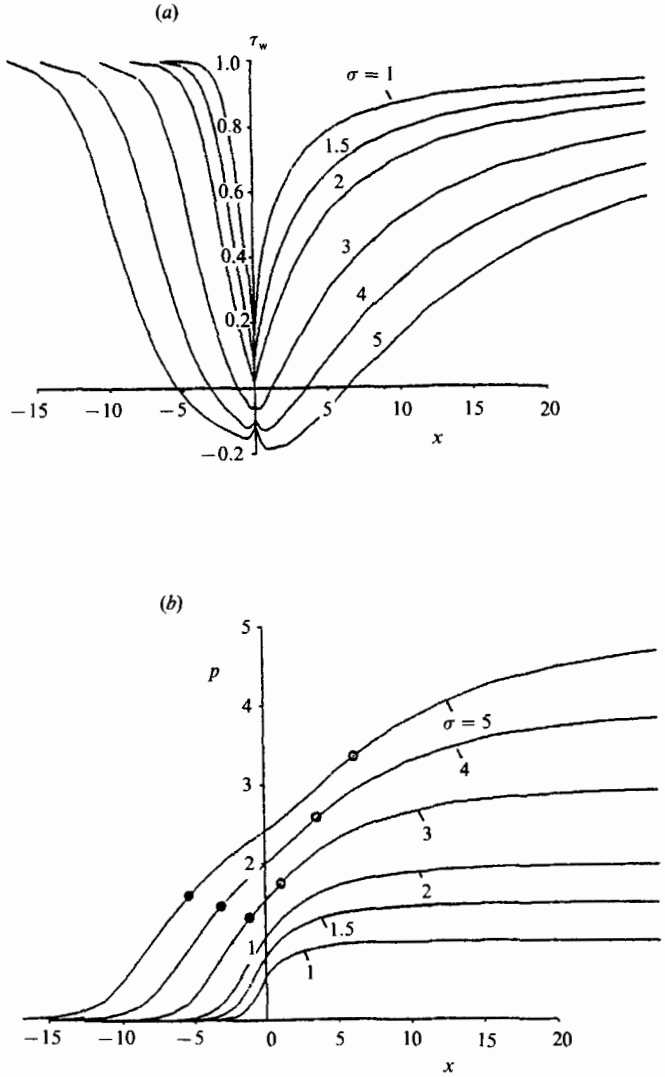

FIGURE 9. (*a*) Ramp-induced wall shear and (*b*) pressure at subcritical wall temperatures corresponding to $\nu = 1$ and $\sigma = 1$, 1.5, 2, 3, 4 and 5 at a reduced ramp angle $\alpha = 1$. Note that the filled and open circles denote the separation and reattachment points, respectively.

interaction zone and for the size of the reverse-flow region, with a significantly different behaviour of wall shear around the corner ($x = 0$).

In an earlier study by Werle & Vatsa (1974), an IBL method was developed and applied to the compressive ramp interaction problem at $Re = 10^4$, 10^6 and 10^8 in a Mach-three flow. The physical ramp angle was so chosen at each Re to give the same reduced ramp angle $\alpha = 2.50$ (for $T_w/T_0 = \frac{1}{2}$, $\gamma = 1.40$). Thus the IBL results, when suitably expressed in the lower-deck variables, can be compared directly with the data of figure 11 (for $\alpha = 2.5$, $\sigma = 1$, $\nu = 0$), assuming that the departure from the classical triple-deck theory is small. This comparison is made in figure 12 for the pressure when the solid curve based on the triple-deck solution of Rizzetta *et al.* (1978) and the dots from the present program are transferred directly from figure 11

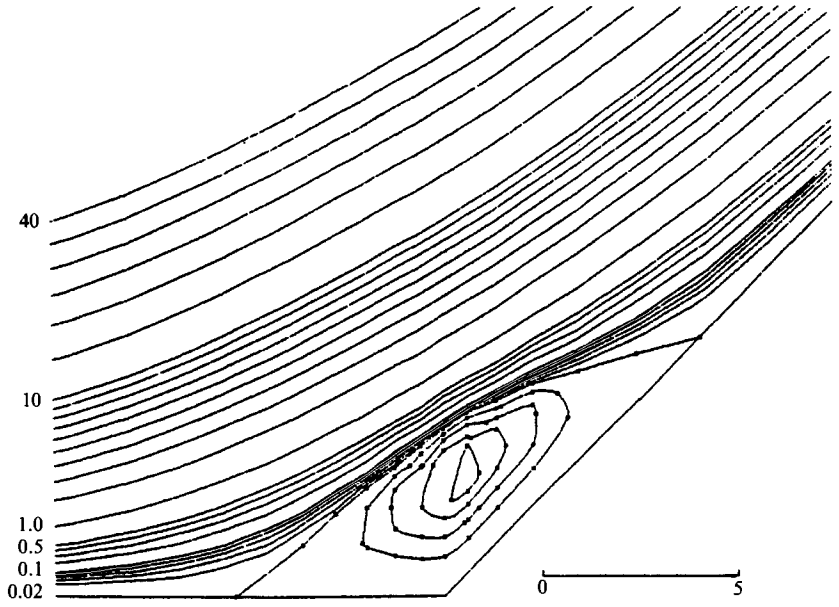

FIGURE 10. Streamline pattern with separation bubble corresponding to figure 9 for $\nu = 1$ and $\sigma = 5$. The contours are drawn in the reduced, lower-deck, boundary-layer coordinates.

unchanged, while Werle–Vatsa's three sets of IBL solutions (Werle & Vatsa 1974) are traced as dashed curves. The encouraging agreement of the present triple-deck result computed for $\nu = 0$ and $\sigma = 1$ with the interactive boundary-layer solution at $Re = 10^8$ should not be too surprising, since ν is expected to be sufficiently small at this Reynolds number, and the agreement attests to the fact that the triple-deck theory represents correctly the asymptotic limit $Re \to \infty$ of the Navier–Stokes solution. Thus the discrepancy between results of Rizzetta *et al.* (1978) (the continuous solid curve) and the IBL solution at $Re = 10^8$ should not be taken as an indication of the need to consider Re values far exceeding 10^8. Estimates of the magnitude of ν at Re of 10^8 and 10^6 in this case indicates that $\nu = 0.37$ at $Re = 10^8$ and 0.66 at $Re = 10^6$. The change in the pressure P resulting from increasing ν from zero to unity has been given in figure 5(*b*), from which one may infer the amount of reduction in P due to the non-vanishing $\nu = 0.37$ and $\nu = 0.66$. One may conclude from figure 5(*b*) that the correction in P at $Re = 10^8$ is quite small and the lowering of P due to $\nu = 0.66$ at $Re = 10^6$ is noticeable, though small, and is in the right direction. The larger amount of reduction in the IBL solution at $Re = 10^6$ from that at $Re = 10^8$ seen in the graph may well be attributed to the weak global interaction unaccounted for in the triple-deck theory and other second-order effects owing to an M_1 not as high as required by the present theory.

3.5. *Effect of wall-temperature reduction*

As mentioned, the separation bubble size and plateau pressure (in lower-deck variables) appear to increase with σ. However, the physical dimensions of the triple deck and the bubble, and the magnitude of the perturbation pressure, actually reduce with increasing σ, i.e. with decreasing wall temperature, as one may anticipate. This follows most directly from the explicit dependence on s_w in (2.66)–(2.68) for the transcritical and subcritical ranges (for which $\nu = 1$).

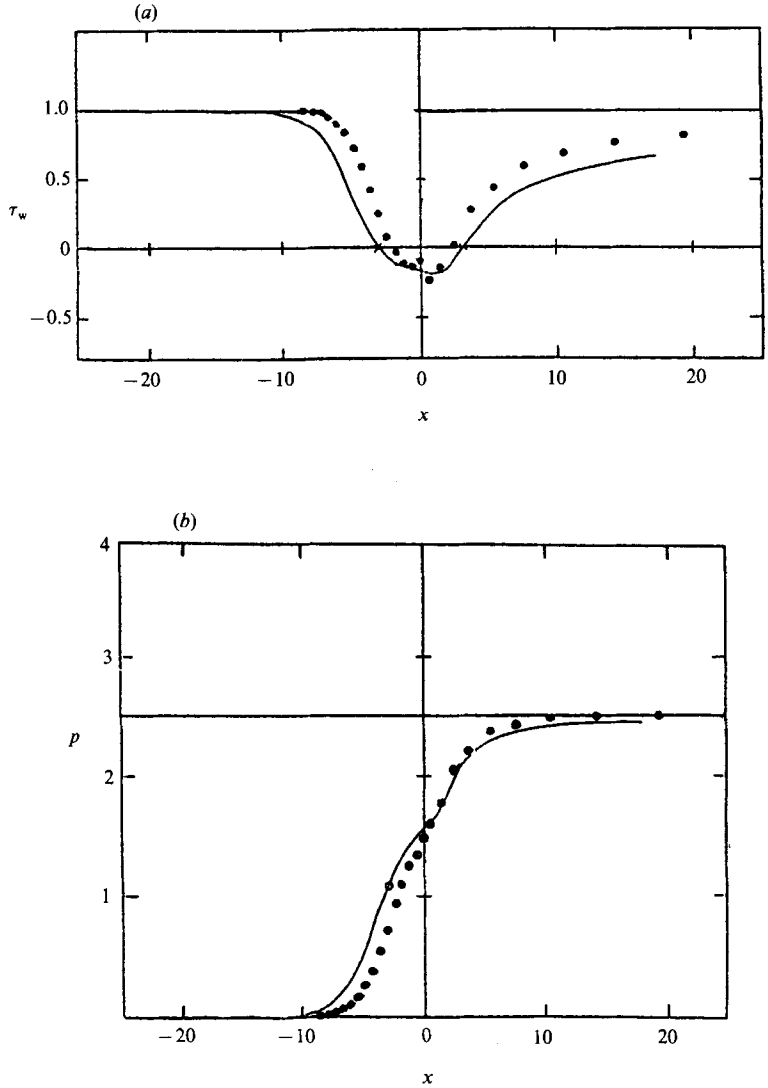

FIGURE 11. Comparison of numerical solutions to the ramp-induced triple-deck problem obtained from an earlier study by Rizzetta *et al.* (1978) (solid curves) and from the present study (dots) at a sufficiently high wall temperature corresponding to the supercritical limit $\nu \to 0$, at a reduced ramp angle $\alpha = 2.5$: (*a*) wall shear, (*b*) wall pressure.

Although the upstream influence diminishes with reducing s_w or T_w/T_0, it is not immediately clear if reducing s_w (at a fixed χ and α^*) can avoid separation; this issue calls for an examination of the solution's dependence on α and σ. Note that α, being a normalized ramp angle, decreases with decreasing s_w like $s_w^{2\omega+1}$ for a fixed χ_0 and α^*, according to (2.66)–(2.68) and (3.5), and that σ increases with decreasing s_w like $s_w^{-(4\omega+2)}$ in the transcritical and subcritical ranges. The numerical solutions obtained in figure 9 for the transcritical and subcritical ranges shows that separation occurs for σ greater than a value between 2 and 3. Now, if the wall temperature is reduced so that α is decreased to one half of its original value in figure 9, then the corresponding σ will increase to four times its original value, that is, σ becomes 8 and 12 if the original σ values are 2 and 3, respectively. But according to the results for $\alpha = 0.5$

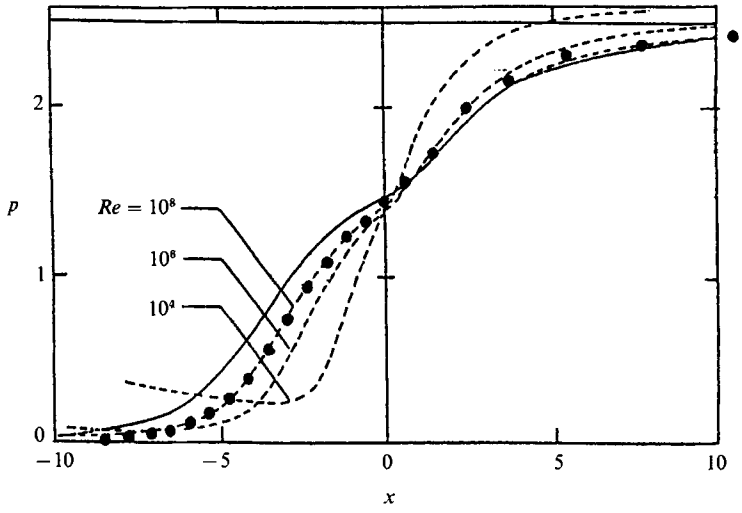

FIGURE 12. Comparison of the numerical results for the ramp-induced pressure obtained from the present analysis (dots) to the IBL solutions obtained earlier by Werle & Vatsa (1974) for $M_1 = 3$, $T_w/T_0 = 0.5$ and $Re = 10^4$, 10^6 and 10^8 at the reduced ramp angle $\alpha = 2.5$ (dashed line). The triple-deck results obtained earlier by Rizzetta *et al.* (1978) are also reproduced (solid curves).

($\nu = 1$) presented in figure 7, the separation appears to occur for a σ between 5 and 10, being rather close to $\sigma = 10$, indicating that separation may very well occur at σ between 8 and 12 The foregoing examination of the available data in this particular case indicates that decreasing s_w cannot effectively eliminate/delay separation, but its upstream influence will drastically reduce with reducing s_w. Nor can one conclude that reducing the wall temperature can provoke separation in an effective manner.

Next we may also point out that, according to (2.68) and (2.69), the streamwise lengthscale of the triple deck will reduce with decreasing s_w like $s_w^{\omega+\frac{1}{2}}$ (at a fixed χ_0) in the supercritical range corresponding to Stewartson's original theory, and will diminish with decreasing s_w like $s_w^{4\omega+2}$ in the transcritical and subcritical ranges (for which $\nu = 1$). Therefore, at a low wall temperature belonging to the latter ranges, the classical theory overpredicts the extent of Δ, hence the extent of upstream influence, by a factor of $s_w^{-3(\omega+\frac{1}{2})}$.

4. Concluding remarks

We have presented an analysis of inviscid–viscous interaction on the triple-deck scales in a hypersonic boundary layer. Although the study focuses principally on the significant influence of a low wall temperature, the work includes the hypersonic version of the original triple-deck theory (Stewartson 1974) in the limit $\chi \to 0$ and $\nu \to 0$ and delineates the departure brought on by wall cooling. As an asymptotic theory, the work may be considered to be of interest for the identification of a characteristic wall-temperature level T_w^*, or s_w^*, and the three distinct wall-temperature ranges relative to s_w^*, representing different degrees of departure from the classical triple-deck theory.

The resulting formulation mathematically shares its reduced governing equations with those of Brown *et al.* (1975) based on a Newtonian strong shock approximation. The latter requires $\gamma \to 1$ for an unrestricted χ, whereas $\gamma \neq 1$ but $\chi \ll 1$ in the present

approach. The underlying reason for the critical influence of wall temperature is attributed to a very special property of the perturbed temperature profile in the main deck, which makes the change in the main-deck displacement thickness in direct proportion to the wall-temperature ratio s_w. Thus at a low s_w, the pressure perturbation may rank equally as a leading contributor to the main-deck displacement, resulting in a significant departure from the original theory. Apart from relaxing the requirement $\gamma \to 1$, the present formulation allows a nonlinear viscosity–temperature law, which should describe more appropriately the lower-deck behaviour and scaling at low wall temperature. Interestingly, the characteristic wall-temperature level s_w^* turns out to be not excessively low for the ranges of χ and γ of practical interest, making the trans- and subcritical domains and their effects more readily realizable.

A more recent study by V. Ya. Neiland (1989, private communication) also addresses a transcritical wall temperature effect. However, its relation to the present analysis remains to be reconciled. As noted in the text, two higher-order effects associated with the normal pressure gradient and with the nonlinear corrections omitted here may yet rank as leading contributors at a still lower wall temperature.

The numerical procedures developed have provided solutions for compressive free interaction and ramp-induced separation and reattachment. Within the ranges of σ or ν considered, the solution accuracy proves to be sufficient to reveal details and features not too clearly brought out in earlier work for the lower supersonic range. Unlike conclusions from earlier studies, the interactive-boundary-layer solutions with separation and reattachment (Werle & Vatsa 1974) at $Re = 10^8$ are shown to closely approach the triple-deck solution from the present numerical study; while the discrepancy at $Re = 10^6$ is yet to be understood, a noticeable part of it may be attributed to the transcritical effect. Contrary to common belief, examination of the available numerical results indicates that separation cannot be prevented/delayed effectively by merely lowering the wall temperature, but the thickness and the length scale Δ of the lower deck, and hence the upstream influence, are drastically reduced. As indicated in the text, further improvement in the convergence characteristic of the relaxation procedure is necessary for the calculation at reduced ramp angles beyond 2.5. The wall-cooling effect on an unsteady triple-deck flow may be expected to be similarly critical, but its influence on hypersonic boundary-layer stability remains to be investigated.

We would like to acknowledge the helpful discussions with O. R. Burggraf, M. M. Hafez, R. E. Melnik, and F. T. Smith on several phases of our work. The study was supported by NASA-DOD Grant number NAGW-1061 and AFOSR Grant number AFOSR-88-0146.

REFERENCES

Bogdonoff, S. M. & Hammitt, A. G. 1956 *J. Aero Sci.* **23**, 108.

Brown, S. N., Cheng, H. K. & Lee, C. J. 1989 *University of Southern California Dept. Aerospace Eng. Rep.* USCAE 148. (Superceeding a paper of the same title in the *Proc. Conf. Prediction and Exploitation of Separated Flows, Roy. Aero. Soc. London, April 18–20, 1989.*)

Brown, S. N. & Stewartson, K. 1975 *Q. J. Mech. Appl. Maths* **28**, 75.

Brown, S. N., Stewartson, K. & Williams, P. G. 1975 *Phys. Fluids* **18**, 633.

Cheng, H. K., Hall, G. J., Golian, T. & Hertzberg, A. 1961 *J. Aero. Sci.* **28**, 353.

Gajjar, J. & Smith, F. T. 1983 *Mathematika* **30**, 77.

HAYES, W. D. & PROBSTEIN, R. F. 1959 *Hypersonic Flow Theory*. Academic.

JENSON, R. 1977 Ph.D. dissertation, the Ohio State University.

KLUWICK, A. 1987 *Z. Angew. Math. Mech.* **67**, 4.

LIGHTHILL, M. J. 1953 *Proc. R. Soc. Lond.* A **217**, 478.

MESSITER, A. 1979 *Proc. 8th US Natl Appl. Mech. Congr., Los Angeles, Ca, USA*.

MOORE, F. K. 1964 *The Theory of Laminar Flow* (ed. F. K. Moore), p. 439. Princeton University Press.

NEILAND, V. YA. 1969 *Izv. Mekh Zhid Gaza* **4**, 40.

NEILAND, V. YA. 1970 *Akad. Nauk. SSSR* **3**, 19.

RIZZETTA, D. P., BURGGRAF, O. R. & JENSON, R. 1978 *J. Fluid Mech.* **89**, 535.

SMITH, F. T. 1982 *IMA J. Appl. Maths* **82**, 207.

SMITH, F. T. 1986 *Ann. Rev. Fluid Mech.* **18**, 197.

SMITH, F. T. & STEWARTSON, K. 1973 *J. Fluid Mech.* **58**, 143.

STEWARTSON, K. 1955 *J. Aero Sci.* **22**, 303; also see *Theory of Laminar Boundary Layer in Compressible Fluids*. Oxford University Press (1964).

STEWARTSON, K. 1974 *Adv. Appl. Mech.* **14**, 146.

STEWARTSON, K. 1981 *SIAM Rev.* **23**, 308.

STEWARTSON, K. & WILLIAMS, P. G. 1969 *Proc. R. Soc. Lond.* A **312**, 181.

STEWARTSON, K. & WILLIAMS, P. G. 1973 *Mathematica* **20**, 98.

SYCHEV, V. V. 1974 *Izv. Akad. Nauk. SSSR, Mekh. Zhid. Gaza* **3**, 47; translated in *Fluid Mechanics*. Plenum Press (1974).

SYCHEV, V. V. 1987 *Asymptotic Theory of Separated Flow* (in Russian), Moscow Science Pub. Physico-Math. Literature. (Distributed by USSR Nat. Comm. Theor. Appl. Mech.)

WERLE, M. J., DWOYER, D. L. & HANKEY, W. L. 1973 *AIAA J.* **11**, 525.

WERLE, M. J. & VATSA, V. N. 1974 *AIAA J.* **12**, 1491.

WILLIAMS, P. G. 1965 *Proc. 4th Intl Conf. Num. Methods in Fluid Dyn.* Lecture Notes in Physics, vol. 35, p. 445. Springer.